Geomorphology 305 (2018) 185–208

Contents lists available at ScienceDirect

Geomorphology

journal homepage: www.elsevier.com/locate/geomorph

Stability and instability on Maya Lowlands tropical hillslope soils

Timothy Beach [a,*], Sheryl Luzzadder-Beach [a], Duncan Cook [b], Samantha Krause [a], Colin Doyle [a], Sara Eshleman [a], Greta Wells [a], Nicholas Dunning [c], Michael L. Brennan [d], Nicholas Brokaw [e], Marisol Cortes-Rincon [f], Gail Hammond [g], Richard Terry [h], Debora Trein [a], Sheila Ward [i]

[a] University of Texas at Austin, United States
[b] Australian Catholic University, Australia
[c] University of Cincinnati, United States
[d] Brennan Exploration, United States
[e] University of Puerto Rico-Río Piedras, United States
[f] Humboldt State University, United States
[g] University College London, United Kingdom
[h] Brigham Young University, United States
[i] Mahogany for the Future, Inc., United States

ARTICLE INFO

Article history:
Received 15 May 2017
Received in revised form 26 July 2017
Accepted 27 July 2017
Available online 29 July 2017

Keywords:
Maya Lowlands
Catenas
Hillslope soils
Geoarchaeology

ABSTRACT

Substantial lake core and other evidence shows accelerated soil erosion occurred in the Maya Lowlands of Central America over ancient Maya history from 3000 to 1000 years ago. But we have little evidence of the wider network of the sources and sinks of that eroded sediment cascade. This study begins to solve the mystery of missing soil with new research and a synthesis of existing studies of tropical forest soils along slopes in NW Belize. The research aim is to understand soil formation, long-term human impacts on slopes, and slope stability over time, and explore ecological implications. We studied soils on seven slopes in tropical forest areas that have experienced intensive ancient human impacts and those with little ancient impacts. All of our soil catenas, except for one deforested from old growth two years before, contain evidence for about 1000 years of stable, tropical forest cover since Maya abandonment. We characterized the physical, chemical, and taxonomic characteristics of soils at crest-shoulder, backslopes, footslopes, and depression locations, analyzing typical soil parameters, chemical elements, and carbon isotopes ($\delta^{13}C$) in dated and undated sequences. Four footslopes or depressions in areas of high ancient occupation preserved evidence of buried, clay-textured soils covered by coarser sediment dating from the Maya Classic period. Three footslopes from areas with scant evidence of ancient occupation had little discernable deposition. These findings add to a growing corpus of soil toposequences with similar facies changes in footslopes and depressions that date to the Maya period. Using major elemental concentrations across a range of catenas, we derived a measure (Ca + Mg) / (Al + Fe + Mn) of the relative contributions of autochthonous and allochthonous materials and the relative age of soil catenas. We found very low ratios in clearly older, buried soils in footslopes and depressions and on slopes that had not undergone ancient Maya erosion. We found high (Ca + Mg) / (Al + Fe + Mn) values on slopes with several lines of evidence that suggest relative youth, soils possibly formed since Maya abandonment. Carbon isotopes ($\delta^{13}C$) also provide some evidence of past vegetation change on slopes. We found strong evidence for maize or other alien C_4 species in an ancient terrace soil and additional evidence in buried footslopes but only evidence for C_3 species (like tropical trees) on the backslopes and other crest-shoulders. The fact that steep slopes preserved no evidence of C_4 species inputs may mean that the ancient Maya maintained forests here. Alternatively, ancient Maya land uses eroded slopes, with the $\delta^{13}C$ signatures detected today being the result of more recent soil development under forest over the last millennium. Additional evidence that these soils are recent in age includes elevated (Ca + Mg) / (Al + Fe + Mn) values, skeletal soil profiles, and low soil magnetic susceptibility. Besides the evidence for truncating backslopes and aggrading footslopes, the ancient Maya built agricultural terraces that accumulated soils and altered drainage. All these ancient Maya slope alterations would have influenced modern tree distributions, because many tree species in the modern forest show strong preferences for different soil types and topographic situations that the ancient Maya changed.

* Corresponding author.
E-mail address: beacht@austin.utexas.edu (T. Beach).

http://dx.doi.org/10.1016/j.geomorph.2017.07.027
0169-555X/

1. Introduction

An enduring question of resilience in biogeomorphic systems is the pace of soil erosion and soil formation during and after periods of intensive human alteration. Maya history—through a long and complex interaction with its tropical, forested slopes—provides a fitting laboratory for addressing such questions. Humans roamed the Maya Lowlands of the Yucatan Peninsula and adjacent areas (Fig. 1) since the late Pleistocene, but the earliest evidence for human impacts on the Maya tropical forest comes from the mid-Holocene. Palynological data from lake cores show declining tree pollen and the first appearance of introduced maize along with disturbance and herbaceous pollen around 5000 years ago (Pohl et al., 1996). From about 3000 to 1000 or 500 years ago, the Maya developed an advanced society, built many cities, and expanded agriculture over a vast area that greatly altered slopes—in destructive and constructive terms (Beach et al., 2015a; Dunning et al., 2015a). The Maya also experienced historical declines after ca. 1750 BP in the Terminal Preclassic (Dunning et al., 2012), rapid growth in the Classic from 1700 to 1100 BP, and the widespread decline or 'Collapse' of the Terminal Classic after ca. 1100 BP (Adams et al., 2004; Luzzadder-Beach et al., 2012; Turner and Sabloff, 2012; Valdez and Scarborough, 2014). Multidisciplinary scientific teams have studied Maya impacts mostly from lake and wetland cores with sedimentation as a proxy for slope erosion. Most such studies indicate forest regrowth after 1000 BP (Mueller et al., 2010) but others interpret continued human impacts in the form of disturbance taxa and charcoal deposition in their cores up to as recent as 210 BP (Wahl et al., 2016). Beach et al. (2015a) and Dunning et al. (2015a) reviewed several studies that revealed evidence for erosion in soil catenas and many studies that have investigated slope management through agricultural terracing. Here we consider six new soil catenas and a new well-dated footslope to understand their formation and their evidence for long-term erosion and ancient management. We then compare these with a synthesis of research on other catenas and depositional soils (behind terrace walls and in alluvial fans, deltas, and footslopes) in this region to show their periods of stability and instability.

The new soil catenas in this study include five sequences on or from backslope gradients of 14–22° under pioneer forest with no evidence of deforestation since the Maya Terminal Classic, about 1000 years ago (Fig. 1). One other sequence occurred near an ancient village (Tulix Mul) on a lower gradient slope of 7–2°, cleared a few years before our field study. For comparison, we also studied another footslope profile below a 20° gradient, pioneer-forest slope. Ancient land uses on the old growth slopes range from the edge of the large ancient Maya city (La Milpa), to the edge of an ancient Maya village (DHGC 950N), to a slope away from a village under old growth (Chawak But'o'ob), and to a slope with little evidence of ancient habitation under old growth (DHGC 1600W).

2. Alluvial, lacustrine, colluvial evidence

This study seeks to characterize soil sequences to understand slope formation over time, especially what evidence the soils may provide

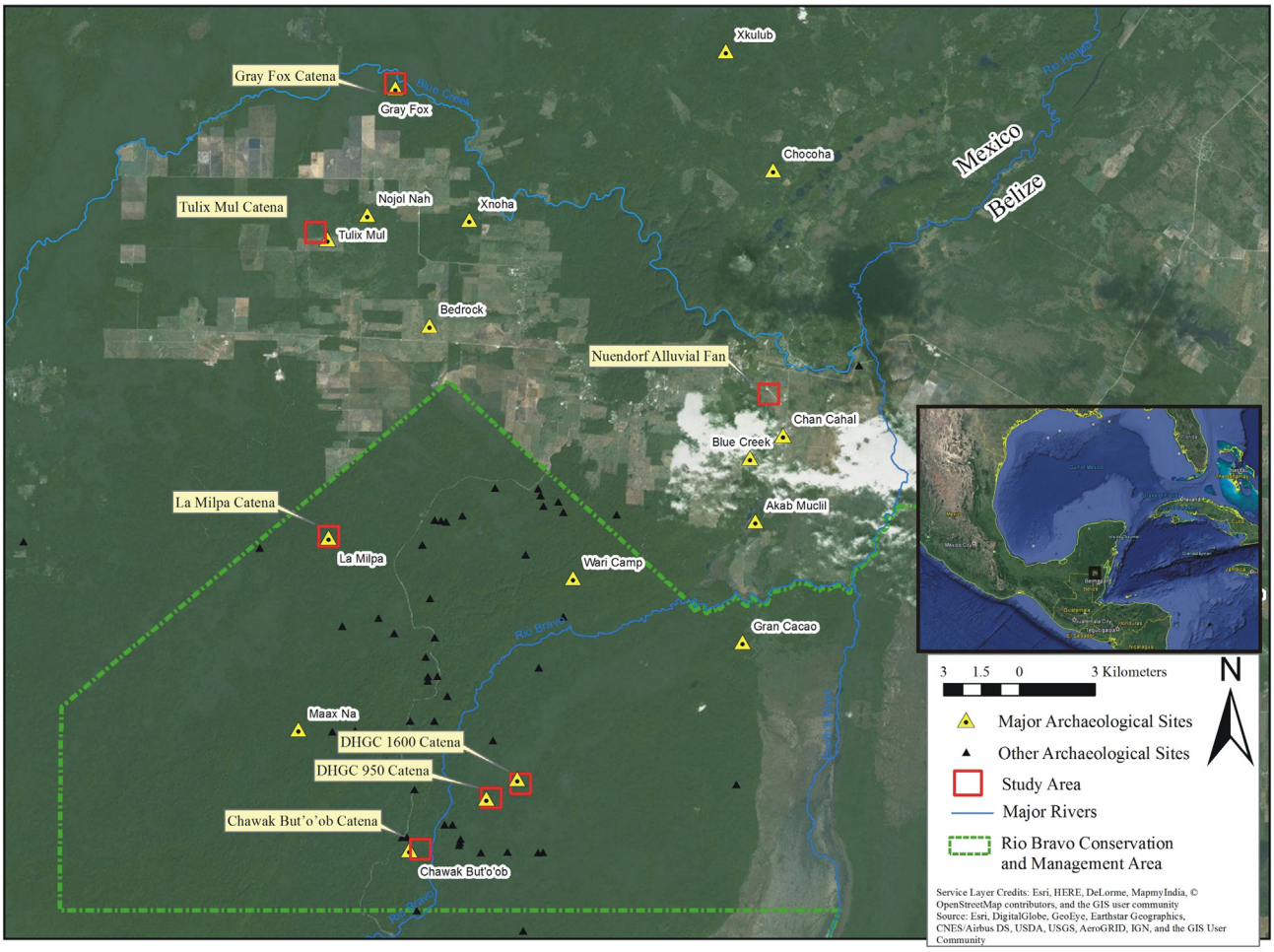

Fig. 1. Sites in the study area and other localities referenced in the study. Study sites are outlined in boxes and include La Milpa, Tulix Mul, Grey Fox, Neundorf, DHGC 959 and 1600, and Chawak.

about the factors of slope erosion over time. Previous work has indicated slope instability associated with increased deposition in lakes, wetlands, depositional basins, ancient reservoirs, floodplains, and catenas, including their colluvial slopes (Dunning and Beach, 2000; Beach et al., 2008, 2009, 2015a, in press; Cabadas-Báez et al., 2010; Dunning et al., 2015a). Many studies referred to sediment that had accumulated over periods of ancient Maya history as 'Maya clays' (Deevey et al., 1979) because clay often dominated the lake deposits dated to the ancient Maya period from ca. 3000 to 1000 BP (calibrated radiocarbon years). For example, a lake coring project from the Petén of Guatemala, close to our study area in geographic and historical terms, indicated that 7 of the 10 m of Holocene deposition was 'Maya clay' associated with Maya land use changes from 4000 to 1000 BP (Anselmetti et al., 2007).

Beach et al. (2008) synthesized the studies that recounted ancient Maya-induced erosion and sedimentation in hillslope, fluvial, and karst sinks. Given that many of these deposits are also clay textures, because the region's soils are dominantly clays, studies often lumped aggradation events with the term 'Maya clays' even though some have coarser textures. These studies used depositional changes, often above buried soils from multiple profiles, to differentiate periods of instability and stability. Studies since 2008 discovered more such aggraded deposits dated to the ancient Maya periods, but only one study focused on alluvial sediments in floodplains and fluvial terraces (Beach et al., 2015b). Aggradation rates in these floodplains and fluvial terraces from ca. 3000–1700 BP in the Maya Preclassic period ranged from 0.82 to 1.5 mm y^{-1} but changed from ca. 2300–1000 BP to 0.98–2.03 mm y^{-1} in the Late Preclassic through Classic periods. During just the Maya Classic period from ca. 1700–1000 BP, aggradation rates ranged from 1 mm y^{-1} to as high as 9.12 and 16.27 mm y^{-1} at ancient Maya wetland field sites on floodplains (Beach et al., 2015b). After ancient Maya abandonment a millennium ago, aggradation declined and surfaces grew more stable as topsoil formation prevailed (Beach et al., 2015a).

Ancient Maya reservoir deposition provides more evidence of Maya impacts on soils and erosion (Akpinar-Ferrand et al., 2012), including a large reservoir at El Zotz in Guatemala's Petén District that aggraded by 2.2 m from ca. 1730 to ca. 1000 BP over a well-constructed floor. This produced a deposition rate of 2.4 mm yr^{-1} from ca. 1730 to ca. 1200 BP in the Late Classic period that dropped to 0.7 mm yr^{-1} from the Late Classic to the present (Beach et al., 2015c; Luzzadder-Beach et al., 2017). Similar to floodplains, reservoir deposits had well-developed topsoils indicative of relative stability since the Late Classic period.

Other foci of geomorphic instability studies have included footslopes, fans, and deltas. Beach et al. (2015a, Fig. 12) developed a conceptual landscape model of slopes that experienced erosion, showing slope instability and agricultural terrace-induced slope stability correlated with the ancient Maya period. In both cases, footslopes, fans, and deltas aggraded during ancient Maya history, whereas terraced slopes preserved more soil from decreased erosion and more deposition from upslope and possibly from ancient human transport of soils from nearby wetlands (Beach et al., in press). Previous footslope, fan, and toeslope studies at Cancuen, Guatemala (Beach et al., 2006; Cook et al., in press); Chan Cahal, Belize (Luzzadder-Beach and Beach, 2009); RB73, Chawak But'o'ob, and Crocodile Lake, Belize (Beach et al., in press); La Milpa, Belize (Dunning and Beach, 2000; Dunning et al., 2003); Guijarral, Belize (Dunning et al., 2009); and Tikal, Guatemala (Dunning et al., 2015b) indicated slope instability (increased deposition from upslope) dated again to the ancient Maya period. The timing of deposition varied by the ages of Maya habitation with clear periods of instability in the Late Classic at Cancuen and Chawak, two Late Classic sites, to Preclassic chronologies at Chan Cahal and the nearby Crocodile Lake delta, both with Preclassic and earlier history. Another footslope at RB73 had one AMS date of 3390 to 3250 BP at a depth of 85 cm within a well-developed paleosol buried by sediment with no pedogenesis capped by less well-developed topsoil. Because this was downslope from a Late Classic village (ca. 1300 BP), Beach et al. (in press) hypothesized that most of the sediment above the buried soil was Late Classic deposition. Likewise, the Crocodile Lake delta had two AMS dates that together ranged from 2350 to 1890 BP at 74 and 95 cm in the Late Preclassic period (Table 1). In contrast, millennia-old agricultural terraces on nearby slopes had thick, stable topsoils, implying relative slope stability.

This research documents little-studied parts of Maya tropical forest: the soil system with varying histories of human impacts. Here, a growing group of studies indicates a complex history of Maya-soil-forest interactions. For example, Hightower et al. (2014) also showed that slopes at Caracol, Belize with Maya agricultural terraces had forests that were taller, had fewer gaps, and were more vertically diverse than unterraced slopes. Such studies indicate the long-term, sometimes positive, interactions between Maya land use, soils, and ecosystems.

3. Regional environments

The study area lies in the heart of the Maya Lowlands, which divides the Pacific and Atlantic Oceans by a narrow isthmus. The major tectonic plates that affect Central America are the North American, the Cocos, the Nazca, and the Caribbean. Active orogeny in the Cenozoic occurred between the Cocos and Caribbean plates at the Middle America subduction zone, as well as sinistral shearing and faulting between the Caribbean and North American plates. Carbonate lowlands, almost exclusively of Cenozoic limestone, make up the Yucatan Platform on the northern portions of the Central American subcontinent (Marshall, 2007). This region generally is tectonically passive with elevations that range from ca. 500 masl to sea level, with a great range of groundwater depths. A variety of karst sinkholes (regionally called cenotes, bajos, and rejolladas) are commonplace in this carbonate rock platform (Bundschuh and Alvarado Induni, 2007).

Northwestern Belize lies on the eastern block-faulted coastal plain of the Yucatan Platform. Here, the low-lying coastal plain, karstic depressions, and riverine wetlands trend inland into a series of north-by-northeast trending normal faults with their horst escarpments rising up to 200 masl between graben valleys (Marshall, 2007).

Water quality studies within northwestern Belize indicate that levels of total dissolved solids, calcium, and sulfate (SO_4^{2-}) fluctuate considerably in surface and groundwater (Beach et al., 2015b). These chemical fluctuations within groundwater are of great importance for water use and soils geomorphology. The region has three main zones of water chemistry: rainwater and upland runoff with low dissolved loads, groundwater with higher dissolved loads (especially with Ca^{2+} and SO_4^{2-}), and littoral waters with varying mixtures of sea water. Additionally, this region has a dramatic dry season and drought cycles. To understand these water extremes on Maya history and ecosystems, Luzzadder-Beach et al. (2016) synthesized ancient Maya water management features for water storage and for water quality management.

3.1. Climate

Multiple factors control the seasonality and quantity of precipitation within this region and thus how climate influences soil formation. Climate drivers include variations in the subtropical high pressure zone and the annual migration of the Intertropical Convergence Zone (ITCZ), which together induce a strong rainy season/dry season pattern and tropical storms that can occur throughout the rainy season from June to December (Boose et al., 1994; Luzzadder-Beach et al., 2012). Substantial climate variations in the Pleistocene and Holocene have also been factors in regional soil development. Core records from Lake Petén Itzá, Petén, Guatemala, provide records of pollen, isotopes of microfauna, and zones of clay-, calcium-, and gypsum-rich lake sediments. Studies have used these proxies to reconstruct terrestrial climate for at least the past 85,000 years (Hodell et al., 2008; Escobar et al., 2012). More recent and resolved records, mainly from speleothems, span the

Table 1
AMS dates.

Sample #	Site	Horizon	Depth (cm)	Material	Conventional age BP	$\delta^{13}C$	Calib 7.0 2 σ BP
Beta 391739[a]	RB73 Footslope	Abss	85	Organic sediment	3120 ± 30	−17.0	3390 to 3250
Beta 391741[a]	Croc Lake	Ab	74	Organic sediment	2010 ± 30	−25.0	2035 to 1890
Beta 391740[a]	Croc Lake	2Ab	95	Organic sediment	2030 ± 30	−24.7	2055 to 1900
NOS-116651[b]	Chawak Footslope	C	60	Charcoal	1300 ± 20	−25.9	1183 to 1287
NOS-116652[b]	Chawak Footslope	Ab1	80	Charcoal	1600 ± 20	−24.1	1414 to 1544
NOS-116653[b]	Chawak Footslope	2Ab	108	Charcoal	2360 ± 25	−23.9	2337 to 2458
Beta 382199	Grey Fox 1a	ACss	85	Charcoal	1090 ± 30	−24.7	1060 to 935
Beta 382200	Grey Fox 1a	Acss	100	Charcoal	1120 ± 30	−25.1	1170 to 960
Beta 382196	Grey Fox 1b	Abss	185	Organic sediment	2530 ± 30	−23.7	2745 to 2495
Beta 382197	Grey Fox 1b	Abss	208	Organic sediment	2530 ± 30	−24.4	2685 to 2350
Beta 382198	Grey Fox 1b	Abss	233	Charred sediment	2390 ± 30	−23.8	2490 to 2345
Beta 382208	DHGC 950 Footslope	Ab	65	Organic sediment	2920 ± 30	−23.8	3165 to 2965
Beta 432115	Neundorf Footslope	Ab1	116	Charred material	1740 ± 30	−25.5	1715 to 1565
Beta 431709	Neundorf Footslope	3C	160	Charred material	2090 ± 30	−24.8	2145 to 1990
NOS-116667[c]	Neundorf Footslope	2Ab	180	Charred plant	2690 ± 30	−27.5	2750 to 2499

[a] Published previously in Beach et al. (2015a).
[b] Published previously in Beach et al. (2015b).
[c] Published previously in Beach et al. (2015c).

entirety of Preclassic Maya to modern occupation (Kennett et al., 2012; Douglas et al., 2015; Medina Elizalde et al., 2016).

Multiple paleoclimatological proxy records from the Maya Lowlands demonstrate that very different climate regimes dominated the region during the late Quaternary. The Petén lake record coupled with the Cariaco Basin record provides evidence that at 24,000 years BP during the Late Glacial Maximum (LGM), the Maya Lowlands region experienced drier and colder conditions than today (Escobar et al., 2012). Moist conditions generally prevailed after the LGM until the drying and cooling of the Younger Dryas (12.9–11.6 ka, 1000 years ago), when forest pollen shifted to savanna pollen assemblages. After the Younger Dryas, the climate became wetter and warmer until the mid-Holocene, except for short-term cooling and drying events such as the 8.2 ka Heinrich event (Escobar et al., 2012). Pollen studies suggest that upland forests of the Maya Lowlands became tropical and that the intermittent *bajo* wetlands became wetter with a few perennially wet pockets (Dunning et al., 2015a). With sea-level rise during the Holocene, lower river valleys and depressions of the low-lying coastal plain became inundated (Pohl et al., 1996; Beach et al., 2009).

Micro- and macrobotanical evidence points to maize domestication and diffusion within northern Belize by 5000 cal. YBP (Pohl et al., 1996) and in the Mexican lowlands as early as 7100 cal. YBP (Pohl et al., 2007). Sedimentation in regional lakes increased after 4000 BP with increasing evidence for cultivation. Recent speleothem research provides strong evidence for recurrent drought cycles throughout the late Holocene and during the entirety of Maya occupation within this region, with key drying episodes occurring during the Late Preclassic (~2000 YBP) and during the Terminal Classic to Postclassic Maya transition (~1000 YBP), as well as historic droughts including during the Little Ice Age (Kennett et al., 2012; Luzzadder-Beach et al., 2016; Medina Elizalde et al., 2016).

3.2. Forests and topography

Forest composition and structure vary predictably along catenas in these karst lands (Fig. 2; Wright et al., 1959; Schulze and Whitacre, 1999). Most tree species show soil and drainage preferences, and so soil and drainage characteristics related to topography affect species distributions (Furley and Newey, 1979). Moreover, because soil and drainage affect tree growth, topography also affects forest height.

The available small-scale maps show little variation in soils and vegetation. Field studies, however, indicate that soils are thin, porous, and well drained on hill crests in karst uplands. Rainfall infiltrates the soils and percolates the limestone bedrock and, combined with wind exposure, leaves crest soils relatively dry. Catena soils generally thicken downslope, and the deepest soils at the footslopes and in depressions can store high soil moisture (Furley and Newey, 1979). Farther below the footslopes, slopes disappear into bajos, or karst sinks, which are

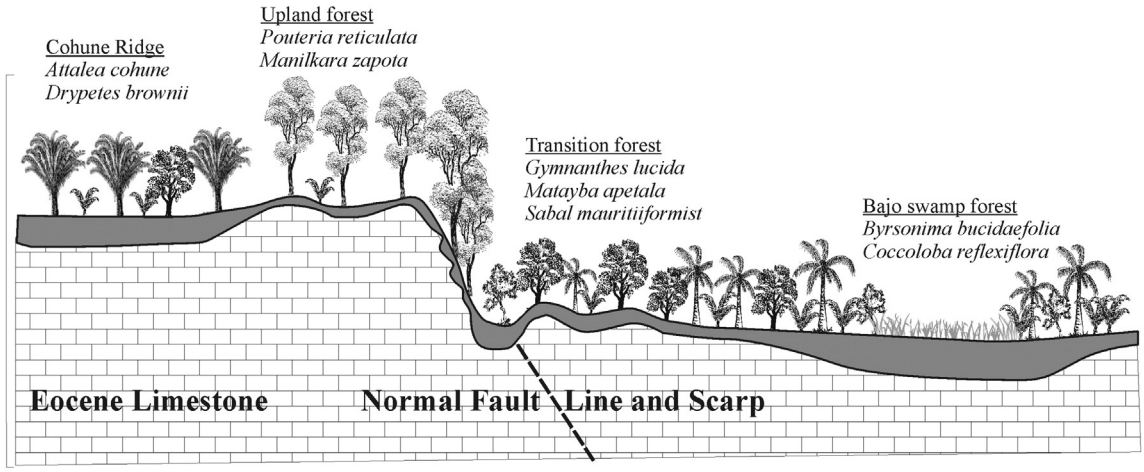

Fig. 2. A topographic catena in northwestern Belize, conceptualizing slope, soil depth, and forest type, including representative tree species. Some 200 or more species are present in these forests. The diagram is adapted from Wright et al. (1959), which they based specifically on their field work in northwest Belize.

flooded in the wet season and, though still moist in the dry season, are then edaphically dry because of strong water retention by the clay soils. The distributions of many tree species and the physiognomy of the forest track these gradients (Fig. 2; Schulze and Whitacre, 1999). The drier, thinner slope soils limit species to only those adapted to periodic dry conditions. Species that occur in the wet bajos, however, must be able to tolerate the extremes of seasonal inundation, edaphic drought, and the churning conditions of Vertisols. Medium height forest grows on crests, taller forests on slopes, medium forests along the transition to bajos, and short, dense, less species-rich forest in bajos. We note that existing, regional vegetation maps cannot show this scale of variation (e.g., Iremonger and Brokaw, 1995; Meerman, 2011).

Many sources indicate that ancient Maya populations were high and land use was intensive especially in the Late Classic (1400 to 1050 BP) in this region up to abandonment about 1050 BP (Hammond et al., 1998). After this time forests regrew and persisted to the present. This history poses questions of how ancient Maya land use has affected the present forest and what we can learn from the present environments about ancient use of specific environments, such as upland bajos and rejolladas, as microclimates for specialized crops (Lentz et al., 2014; Munro-Stasiuk et al., 2014).

3.3. Soils and catenas

Previous soil work in this region has ranged from small-scale government maps of soil resources (King et al., 1992) to larger-scale studies for individual projects to assess farming capability, soil erosion, and geoarchaeology (Beach et al., in press). The soil formation factors (CLORPT: climate, organisms, relief, parent material, and time) in this region include a tropical forest, AF or AM climate with about 1500 mm of rainfall and a distinct dry season from January to June. The soil temperature is hypertropothermic and the soil moisture is Udic, although evapotranspiration is also nearly 1500 mm. The tropical forest here has about 50 tree species per hectare (Brokaw et al., 1993; Brewer et al., 2003). Some savanna vegetation occurs in the region in lowlands that have sandy soils, but none of our soil catenas occur in these areas.

A soil catena is a sequence of soils along a slope. The underlying concept is that a catena holds all other soil-forming factors constant to understand how relief changes soils (Holliday, 1992, p. 252; Jenny, 1994). Such factors include length and gradient of slopes, relief, and drainage as well as aerial inputs (Holliday, 1992, p. 251). These factors lead to differences in rates of erosion and deposition and infiltration and percolation, which affect soil drainage (oxidation and reduction) and translocation (Sommer and Schlichting, 1997). Only a few catena studies are available for this region, including Furley and Newey (1979), Furley (1987), Coultas et al. (1993, 1994, 1997), Beach (1998), Burnett et al. (2012), and Beach et al. (in press).

All catenas in this study occur from ca. 20 to 200 masl on the normal fault-created Rio Bravo and La Lucha escarpments. Lithologies are limestone or dolomitic limestone (Brennan et al., 2013); and the soils here develop from transformations, outputs, and inputs on the slopes. The transformations include various types of weathering, whereas slope inputs occur from upslope, from the distant Saharan dusts, and nearer though upwind Central American volcanoes; but only three studies have begun to quantify allochthonous inputs (Cabadas et al., 2010; Bautista et al., 2011; Tankersley et al., 2016). The outputs include slope erosion, weathering and leaching, and mass wasting with a significant contribution from tree throw (Beach, 1998). On similar slope gradients with old growth forest in the Czech Republic, Phillips et al. (2017) showed that tree throw dominates slope processes.

Thus far, these soil sequences only have AMS dating and date to the late Holocene, though a few buried soils in depressions have dated to the late Pleistocene (Dunning et al., 2009; Beach et al., 2015a). We posit three hypotheses to explain the relative youth of slope soils. First, slope soils may have formed only since the abrupt transition from late Pleistocene wet and dry cycles to Holocene wetness, which may have led to slope stripping. Second, the slope development process from natural formation, erosion, and mass wasting is too fast for materials to persist for long. For example, tropical forest catenas with similar CLORPT factors had high turnover through tree throw in the nearby Petexbatún of Guatemala (Beach, 1998). Third, many slopes may have been stripped during the Maya period of intensive land use from 3000 to 1000 BP. Ancient Maya populations and intensive land uses spread across much of this region during this time. Each of the three hypothetical processes may have prevailed on different slopes in the region because of the varying land uses and slope characteristics over time and place. Further evidence from dating soils on the slopes should allow us to test these hypotheses and expand on the small number of late Holocene ages of footslopes.

Beach et al. (in press) hypothesized from a different group of catena soils in this region that they indicated relatively recent formation. Most sloping soils reflected the geochemistry of bedrock with high amounts of calcium carbonate equivalent ($CaCO_3$), high hydrochloric acid (HCl) reaction reflecting little weathered carbonate, low magnetic susceptibility, low concentrations of metal elements that are rare in the bedrock but increase with time as carbonate leached and metals rained in from allochthonous sources, and coarser soil textures that become finer (clays) with tropical weathering. Beach et al. (2017) also showed many of these same qualities in soils formed since the Maya abandonment around Chunchucmil, Yucatán, Mexico, with about half the precipitation of the present study area. They also found that soil formation of A horizon material above dated surfaces ranged from 0 to 0.15 mm y^{-1} since the Maya Late Classic, which could account for as much as 18 cm of soil formation (ca. 1200 BP) (Beach et al., 2017, p. 206).

The soil parent material in this region has readings of nearly zero magnetic susceptibility, as do young soils formed here because they are dominantly carbonate or have high gypsum with their carbonate. Increased magnetic susceptibility would have to come from increased ferromagnetic minerals that would derive from anthropogenic sources that increase concentrations of magnetically susceptible minerals, other allochthonous inputs, neoformation of magnetically susceptible minerals, or differential weathering that leaves magnetically susceptible minerals and removes carbonates. Each of these pathways imply greater time depth for soil formation. Thus, older and more human-altered soils should have higher magnetic susceptibility. For example, in older, buried soils, $CaCO_3$ levels and HCl reactions were lower, metal elements and magnetic susceptibility increased, and soil textures were finer. Some of the older buried soils also had some iron oxide and manganese oxide masses, some nodules, and vertic features like slickensides and wedge-shaped soil structure. We did not recognize Bt horizons or cutans in the field, though some of the older soils increased in clay content in the lower horizons.

Another line of evidence for relative slope age in this region is the ratio: (Ca + Mg) / (Al + Fe + Mn). Based on total elemental extraction by ICP-MS (inductively coupled plasma mass spectrometry) we use this ratio to compare soil horizons and profiles (Tables 2–6). We hypothesize that high values of (Ca + Mg) / (Al + Fe + Mn) on these slopes should reflect soils that are little altered from their parent material, which is limestone and dolomitic limestone. The soils with high Al + Fe + Mn should reflect greater time of alteration because carbonate minerals weather and dissolve over time; Ca and Mg preferentially leach; and Al, Fe, and Mn build up over time caused by some combination of refining the rare autochthonous quantities and gradual increase of allochthonous sources such as African and North American dusts and volcanic ash (Cabadas et al., 2010; Bautista et al., 2011; Tankersley et al., 2016). We avoided Si in these calculations because Si could derive from chert- or phytolith-rich zones rather than differential weathering or allochthonous sources.

An indirect line of evidence for slope age is the carbon isotopic ($\delta^{13}C$) profile of soils. Pollen evidence suggests forest vegetation (Beach et al., 2015a), virtually all C_3 species, throughout the

Table 2
Chawak catena: field and laboratory soil data (Alluvial fan data partly from Beach et al., 2015b).

Soil profile	Slope	Depth		Horizon	Soil color	Fe, Mn	Clay	Class	$\delta^{13}C$	MS 10^{-3} SI	pH	Organic matter	CEC	Si	Al	Fe	Ca	K	Mg	Mn	P	S	Na	Zn
Great group	°	cm			Moist	Masses nodules	%		%			%	cmol/Kg	mg/Kg	mg/Kg	mg/Kg	mg/Kg	mg/Kg	mg/Kg	mg/Kg	mg/Kg	mg/Kg	mg/Kg	mg/Kg	mg/Kg
Chawak But'o'ob	3.0	0	2	O						0.04															
Crest-Shoulder		2	15	A1	10YR 2/1		31.00	CL	NA	0.06	7.6	11.8	22.3		10,840	3463	171,368	395	19,841	160	406	743	236	14
		15	32	A2	10YR 2/1		19.58	Loam		0.08	7.7	5.4	11.0		6531	1824	162,006	205	23,240	101	233	1746	209	8
Mollisols		32	42	AC	10YR 3/1		22.03	SCL		0.02	7.8	3.8	52.7		7190	1607	174,527	193	27,910	67	186	174	242	7
(Lithic Haprendolls)																								
Chawak But'o'ob	15.0	0	2	O						0.01														
Backslope		2	12	A	10YR 2/1		50.62	Clay	NA	0.06	7.8	5.5	46.6		18,926	6976	144,315	1178	13,528	405	517	993	206	31
Mollisols		12	30	A2	10YR 2/1		33.42	CL		0.08	7.5	15.4	27.5		9173	3710	181,837	742	8929	234	251	512	143	19
(Lithic Haprendolls)																								
Chawak But'o'ob	1.0	0	2	O						0.13														
		2	15	A1	10YR 2/1		84.24	Clay	NA	0.26	7.3	15.5	45.0		14,507	16,004	22,573	284	3577	641	242	628	110	52
Footslope		15	32	A2	10YR 2/1		40.16	Clay		0.24	7.6	4.7	29.3		11,227	9889	146,308	450	8917	514	108	582	98	35
Mollisols		32	40	A3	10YR 3/1		47.19	Clay		0.32	7.8	3.8	41.4		14,148	7940	173,282	661	9407	260	87	191	130	29
(Lithic Haprendolls)		40	47	AC	10YR 4/1		40.43	Clay		0.06	7.6	2.3	46.1		10,244	5375	204,445	793	5583	129	55	232	91	23
Chawak But'o'ob	2.0	0	1	O						0.14														
		1	31	A	10YR 2/1		27.9	CL	−26.8	0.34	7.3	7.4	39.8		23,146	6971	173,851	1008	40,453	997	351	697	246	39
Alluvial fan		31	62	C	10YR 3/2		14.3	CoSL	−25.1	0.25	7.7	4.3	17.9		9805	2774	241,977	499	47,656	316	158	287	255	18
Mollisols		62	80	Ab1	10YR 3/1		23.7	Loam	−23.3	0.30	7.6	6.4	26.6		14,951	4268	271,703	830	40,214	397	230	254	282	24
(Cumulic Hapludolls)		80	99	Ab2	10YR 3/1		28.9	CL	−24.1	0.14	7.6	3.6	26.2		19,741	5705	211,937	838	52,332	381	153	240	269	24
		99	110	Ab3	10YR 3/1		38.4	CL	−25.8	0.08	7.6	3.8	32.0		28,386	8253	208,865	1016	37,080	465	161	206	244	34
		110	125	2C	10YR 5/1		42.1	Clay	−25.8	0.06	7.9	3.2	24.4		20,101	5975	195,219	962	21,790	284	114	141	198	25

Table 3
La Milpa catena: field and laboratory soil data.

Soil profile	Slope	Depth		Horizon	Soil color	Fe, Mn	Clay	Class	$\delta^{13}C$	MS 10^{-3} SI	pH	Organic matter	CEC	Si	Al	Fe	Ca	K	Mg	Mn	P	S	Na	Zn
Great group	°	cm			Moist	Masses nodules	%		%			%	cmol/Kg	mg/Kg	mg/Kg	mg/Kg	mg/Kg	mg/Kg	mg/Kg	mg/Kg	mg/Kg	mg/Kg	mg/Kg	mg/Kg	mg/Kg
La Milpa																									
Crest-Shoulder	3.0	0	1	O						0.06															
		1	12	A	10YR 2/2		23.7	SiL	−26.9	0.13	7.2	11.1	43.4		6560	1943	225,074	476	12,279	329	464	1054	230	11
Mollisols		12	28	A2	10YR 4/2		19.1	SiL	−28.9	0.13	7.8	5.8	22.3		7639	2168	315,387	455	15,284	319	374	725	300	12
(Cumulic		28	40	AC	10YR 4/2		13.5	Loam	−22.9	0.10	7.7	3.7	14.2		6832	2088	328,659	621	14,960	204	306	485	290	14
Hapludolls)		40	70	C	10YR 5/2		22.9	Loam	−28.9	0.07	8.1	1.7	11.0		3685	1236	366,313	298	12,180	114	217	336	295	11
		70	105	Ab-2C	10YR 3/2		32.7	CL	−22.6	0.09	7.9	3.0	17.5		8415	2692	298,977	3073	14,058	199	201	348	272	13
La Milpa																								
Backslope	15.0	0	1	O						0.15														
Mollisols		1	9	A	10YR 2/1		45.9	SiC	−24.9	0.25	7.0	12.8	51.5		35,293	12,732	93,685	2004	9932	789	482	1316	190	47
(Lithic		9	22	A2	10YR 2/1		10.7	SiL		0.27	7.2	10.3	46.1		38,171	14,685	105,838	1797	10,624	830	479	771	188	51
Haprendolls)		22	30	AC	10YR 3/1		25.3	SiL	−26.3	0.22	7.7	6.7	46.1		29,263	10,832	137,258	1467	12,317	640	302	497	185	38
La Milpa																								
Footslope	7.0	0	1	O						0.08														
Mollisols		1	11	A	10YR 2/1		33.1	CL		0.12	7.0	10.5	40.8		19,323	6079	145,314	1802	23,677	641	508	990	198	27
(Lithic		11	22	A2	10YR 2/2		32.3	CL	−25.1	0.13	7.4	6.8	33.9		15,412	4823	201,933	1436	29,890	584	438	760	230	23
Haprendolls)		22	35	AC	10YR 4/2		25.1	Loam	−27.3	0.09	7.5	4.0	19.5		14,331	4427	237,457	1678	45,258	441	350	563	288	22
	2.0	0	1	O						0.19														
La Milpa		1	31	A1	2.5YR 3/1		20.1	Loam	−27.3	0.25	7.4	6.7	29.3		10,589	4206	220,130	1078	22,137	825	499	690	231	24
Sink		31	62	C	2.5YR 5/2		33.9	CL	−26.1	0.23	7.9	3.0	22.3		10,462	3942	208,344	861	17,233	540	199	259	269	22
Mollisols		62	80	Ab/Cg mix	10YR 3/1, 5/1	Mn m	32.3	CL	−25.2	0.65	7.5	5.7	46.1		41,535	19,982	107,092	3151	10,691	7011	181	92	450	66
(Cumulic Hapludolls)		80	99	Cg/mixed	10YR 5/1, 3/1	Mn m	68.5	Clay	−25.1	0.54	7.8	5.8	45.0		21,474	10,161	33,468	1552	4823	2413	93	38	175	35
		99	110	Ab	10YR 3/1	Mn m	65.2	Clay	−24.4	0.59	7.8	6.4	52.7		22,744	11,556	40,641	1529	5283	3731	97	41	173	42
		110	125	2C cobbly clay	10YR 5/1		47.7	Clay	−26.2	0.30	7.7	5.5	41.4		18,780	8087	87,870	1504	12,173	2034	108	81	173	33

Table 4
Grey Fox catena: field and laboratory soil data.

Soil profile	Slope	Depth		Horizon	Soil color	Fe, Mn	Clay	Class	$\delta^{13}C$	MS 10^{-3} SI	pH	Organic matter	CEC	Si	Al	Fe	Ca	K	Mg	Mn	P	S	Na	Zn
Great group	°	cm			Moist	Masses nodules	%		%			%	cmol/Kg	mg/Kg	mg/Kg	mg/Kg	mg/Kg	mg/Kg	mg/Kg	mg/Kg	mg/Kg	mg/Kg	mg/Kg	mg/Kg
	1.0	0	2	O																				
Grey Fox 1A		2	12	A1	7.5YR 2.5/1				−27.9	0.105	6.6	9.7	32.4	1989	29,262	9040	17,150	954	5321	1381	262	200	56	37
Sink		12	56	A2	7.5YR 2.5/1		86	Clay	−26.6	0.131	6.6	7.1		595	31,762	10,026	15,219	942	5305	1186	123	40	60	35
Vertisols		56	71	A3	G1 N6				−25.4	0.149	6.8	6.7		1066	34,368	10,786	15,238	989	5389	1126	106	20	96	39
		71	80	ACss	G1 N6 mottled					0.142	7.8	5.7		5067	32,943	10,278	37,823	1174	5534	1278	80	24	168	40
		80	120	Cgss1	2.5Y 8/1	Mn m				0.108	7.8	4.5		13,038	21,725	5310	123,835	3834	5009	942	68	551	294	30
		120	142	Cgss2	G1 8 10Y	Mn m	48	Clay		0.042	8.4	1.2		1394	6158	930	431,187	66	2793	320	62	578	334	5
	1.0	0	1	O						0.047														
Grey Fox 1B		1	12	A1	7.5YR 3/2		74	Clay	−28.1	0.096	6.3	12.9	35.1	1318	30,764	9312	16,652	313	3993	1198	281	429	193	36
Floodplain		12	40	A2	2.5YR 3/1				−26.7	0.083	5.8	7.1		361	29,969	9058	11,389	280	3338	448	115	32	160	28
Sink		40	55	Abss	2.5YR 3/1				−27.3	0.131	6.4	7.0		231	30,837	9136	12,400	331	3552	274	108	28	178	29
Vertisols		55	150	2Abss	2.5YR 3/1		93	Clay		0.117	8.2	4.5		16,052	23,853	7515	147,389	1152	10,883	493	204	113	533	32
		150	200	3Abss top	7.5YR 3/1				−24.3	0.112	8.4	4.6		4188	21,081	6357	104,794	807	10,142	459	146	95	1397	25
		200	230	3Ab bottom	7.5YR 3/1					0.133	8.2	5.0		14,958	26,043	8033	84,456	917	13,630	256	146	211	1918	30
		230	250	C1	5YR 7/1		71	Clay	−25.1	0.107	8.2	5.1		1008	25,823	7283	69,260	1268	16,325	365	78	241	2057	34
	8.0	0	1	O																				
Grey Fox 1C		12	12	A1	10YR 2/1				−27.9	0.087	6.3	13.3	35.0	4548	28,391	8470	15,988	442	4356	697	303	426	138	36
Footslope		12	40	A2ss	10YR 2/1		87	Clay	−26.0	0.063	6.4	8.9		3503	25,820	7356	14,427	460	3950	495	208	156	178	30
Vertisols		40	80	A3ss	10YR 3/1				−26.4	0.087	6.4	7.5		2085	26,504	7920	12,672	456	3785	474	125	65	190	29
		80	110	ACss	10YR 3/1				−26.7	0.029	7.6	6.6		5076	29,668	9161	16,754	1142	6442	233	107	46	126	36
		110	122	C1ss	10YR 8/2, 5/2 mottled					0.017	8.2	2.4		3230	10,150	2866	314,223	544	18,977	240	75	226	155	12
		122	200	C2	7.5YR 8/2		46	Clay	−27.5	0.013	8.2	1.4		763	5023	1413	348,700	228	64,426	109	75	225	169	4

Table 5
Tulix Mul catena: field and laboratory soil data.

Soil profile	Slope	Depth		Horizon	Soil color	Fe, Mn	Clay	Class	$\delta^{13}C$	MS 10^{-3} SI	pH	Organic matter	CEC	Si	Al	Fe	Ca	K	Mg	Mn	P	S	Na	Zn
Great group	°	cm			Moist	Masses nodules	%		%			%	cmol/Kg	mg/Kg	mg/Kg	mg/Kg	mg/Kg	mg/Kg	mg/Kg	mg/Kg	mg/Kg	mg/Kg	mg/Kg	mg/Kg	mg/Kg
Tulix Muul	2.0-	0	10	Ap	10YR 2/1		49.3	Clay	−25.5	0.06	7.0	12.0	46.6		13,474	4849	13,344	908	2375	688	238	403	44	27
Crest-Shoulder	7.0	12	30	A2	10YR 2/1		44.0	Clay	−26.3	0.11	7.0	3.6	27.5		10,106	4436	7851	358	1470	189	97	123	28	13
		30	50	AC	10YR 3/1		45.5	Clay	−25.3	0.10	7.5	2.3	30.2		11,328	3574	31,320	209	2836	127	71	56	87	15
Mollisols		50	60	C	10YR 7/1, 8/6				−25.9	0.05														
(Hapludolls)		60	75	Cg	10YR 6/1, 8/6	Mn nod	60.9	Clay	−27.1	0.03	7.6	4.0	39.3		12,474	2899	16,762	129	1902	14	49	19	90	10
Tulix Muul	7.0-	0	10	Ap	10YR 2/1		56.5	Clay	−26.1	0.045	7.1	10.1	63.2		17,250	6297	22,774	883	4393	912	298	449	59	26
Backslope	3.5	10	40	A2	10YR 3/1		44.9	Clay	−25.8	0.105	7.5	4.7	33.9		15,146	5103	64,226	529	3078	669	132	98	76	21
Mollisols		40	55	A3	10YR 2/1		51.1	Clay	−27.1		7.4	6.2	48.2		18,753	6180	30,801	564	3041	912	100	52	86	30
(Cumulic		55	65	A3	10YR 3/1		62.1	Clay		0.133	7.5	4.7	44.5		19,363	6784	14,287	578	2345	1215	68	25	55	24
Hapludolls)		65	75	AC	10YR 4/1	Mn, Fe m	53.3	Clay		0.106	7.8	3.9	49.3		16,819	6215	25,537	489	2590	785	86	40	82	24
Tulix Muul	2.0	0	12	Ap	10YR 2/1		59.5	Clay	−24.4	0.1	7.0	9.8	45.5		20,605	7242	19,232	1416	3701	1327	268	410	72	32
Footslope		12	40	A2	10YR 2/1		59.7	Clay	−27.3	0.109	7.1	6.7	45.5		17,981	6117	12,392	625	2738	772	78	74	40	22
Mollisols		40	80	A3ss	10YR 3/1		60.3	Clay	−25.7	0.112	7.3	5.6	45.0		16,264	5396	13,087	655	2461	823	62	26	46	22
(Vertic Hapludolls)		80	110	Css	10YR 5/1, 8/8	Mn, Fe m	38.1	CL	−24.8	0.027	7.8	3.3	37.3		9971	3063	60,518	268	2781	461	51	80	47	10
		110	130	C2 mix C1	10YR 7/1, 8/8		6.5	SiL	−26.3	0.017	8.0	1.4	48.8		6410	1939	308,397	294	15,217	307	79	231	204	10
		130	160	C3 SiS	10YR 7/1, 8/8		5.5	SiL	−26.5	0.008	8.0	1.1	16.4		2393	2239	219,520	132	147,646	311	75	344	589	7

Table 6
DHGC 950 and 1600 catena: field and laboratory soil data.

Soil profile	Slope	Depth		Horizon	Soil color	Fe, Mn	Clay	Class	$\delta^{13}C$	MS 10^{-3} SI	pH	Organic matter	CEC	Si	Al	Fe	Ca	K	Mg	Mn	P	S	Na	Zn
Great group	°	cm			Moist	Masses nodules	%		%			%	cmol/Kg	mg/Kg	mg/Kg	mg/Kg	mg/Kg	mg/Kg	mg/Kg	mg/Kg	mg/Kg	mg/Kg	mg/Kg	mg/Kg
DHGC																								
950	2.5	0	1	O						0.053														
Crest-Shoulder		1	10	A1	5YR 3/1		26	Loam	−26.7	0.053	7.7	10.1	18.0	4061	4612	1377	455,349	250	23,454	288	307	1045	222	7
		10	27	A2	10YR 3/2				−27.5	0.080	7.9	4.5		3416	5882	1783	477,451	121	28,000	254	227	603	211	6
Mollisols		27	40	AC	5YR 4/1				−26.5	0.067	7.8	3.1		5704	4565	1273	501,486	257	26,102	165	197	442	210	5
(Lithic Haprendolls)		40	50	C	10YR 8/2				−26.7	0.038	8.4	0.9		2748	2167	484	571,584	50	18,573	35	80	223	162	4
DHGC																								
950	17.0	0	1	O																				
Backslope		1	11	A1	10YR 2/1				−27.6	0.158	7.5	11.8	23.9	2163	13,693	5227	179,850	407	50,753	904	321	916	165	50
Mollisols		11	22	A2	10YR 2/1		22	Loam	−27.5	0.224	7.9	5.8		1002	9901	3697	281,536	171	65,589	609	207	483	171	14
(Lithic Haprendolls)		22	30	AC	10YR 3/1				−27.1	0.218	7.8	4.4		773	8645	3160	332,306	148	56,336	510	185	412	172	13
	1.0	0	1	O						0.207														
DHGC		1	12	A1	10YR 2/1		58	Clay	−28.5	0.335	6.9	8.1	27.5	699	31,026	1290	11,228	156	6706	2346	132	154	60	32
950		12	20	A2	10YR 3/1				−27.1	0.400	7.0	7.3		777	29,423	12,075	9340	133	6187	1892	98	88	50	32
Footslope		20	32	A3	10YR 3/1				−26.3	0.238	7.3	7.0		754	28,854	11,766	10,336	164	6584	1907	95	74	57	37
Mollisols		32	42	A3	10YR 3/1				−26.8		7.7	6.3		1343	27,660	11,073	32,346	118	14,477	1702	93	80	74	29
(Cumulic Hapludolls)		42	50	Ab	10YR 3/1				−26.4	0.285	7.6	6.2		2746	26,309	10,462	21,610	113	10,128	1600	79	52	69	30
		50	64	Ab	10YR 2/1		64	Clay	−26.3	0.251	7.9	5.5		9445	21,643	8528	40,911	155	8712	1922	71	63	71	42
		64	75	C	10YR 8/2				−27.5	0.044	8.3	2.5		9640	10,605	3215	255,266	67	26,748	1387	48	203	140	15
DHGC																								
1600	3.0	0	1	O																				
Crest-Shoulder		1	9	A1	10YR 2/1		22	Loam	−28.9	0.042	7.4	20.0	26.7	1632	7592	2851	233,332	228	19,901	285	294	1294	149	13
		9	26	A2	10YR 2/1				−27.4	0.057	7.8	6.1		1091	5405	1922	415,575	115	33,921	225	179	581	185	10
Mollisols		26	40	AC	10YR 3/1				−27.0	0.047	8.0	3.5		1641	4254	1476	467,566	37	25,002	141	147	388	158	4
(Lithic Haprendolls)		40	45	C	10YR 3/2					0.031	8.3	1.7		4184	2757	870	511,130	2	21,398	64	96	235	148	2
DHGC																								
1600	22.0	0	1	O						0.042														
Backslope		1	9	A1	10YR 2/1				−27.7	0.057	7.5	11.0	22.9	578	12,979	6212	163,165	336	55,763	577	281	824	202	19
Mollisols		9	25	A2	10YR 3/1		53	Clay	−26.9	0.047	8.0	4.8		8474	12,146	6572	332,811	228	70,248	545	262	535	249	16
(Lithic Haprendolls)		25	42	AC	10YR 3/2				−26.7	0.031	8.0	4.0		5831	7866	3915	305,071	137	70,194	310	190	412	240	9
DHGC	3.0	0	1	O						0.292														
1600		1	15	A1	10YR 2/1		37	SiCl	−27.8	0.426	7.3	13.6	32.8	2531	28,879	13,686	27,073	443	11,786	973	311	658	80	37
Footslope		15	30	A2	10YR 3/1			Clay	−26.8	0.457	7.7	8.1		1867	22,332	9633	97,991	313	42,007	666	196	375	138	26
Mollisols		30	40	A3	10YR 3/1			Clay	−25.3		7.8	7.3		3629	33,939	14,916	68,756	427	22,097	864	185	206	100	40
(Cumulic Hapludolls)		40	60	AC	10YR 4/1					0.090	8.5	2.4		6452	11,072	4728	215,058	169	71,273	280	95	181	197	12
		60	70	C	10YR 8/3					0.056	8.5	1.9		4664	6459	2804	351,142	89	57,325	160	87	234	186	6
	1.0	0	1	O																				
DHGC		1	11	A1	10YR 2/1				−28.5	0.268	6.6	11.9	27.1	5961	24,941	11,366	12,186	172	4204	1242	213	439	45	29
1600		11	24	A2	10YR 3/1		53	Clay	−26.8	0.373	7.0	7.3		1971	30,132	13,261	9046	178	4816	1148	113	102	66	35
Sink		24	39	A3	10YR 3/1				−26.1	0.326	6.3	6.2		1214	27,738	12,715	8297	132	4752	959	100	60	65	28
Vertisols		39	45	A3	10YR 3/1				−25.7	0.295	6.0	5.9		1585	25,073	11,462	6989	106	4275	933	75	29	74	24
		45	55	Acss	10YR 3/1	Mn m	66	Clay	−24.7	0.252	5.7	5.8		4619	26,490	12,451	7146	132	4579	936	76	25	81	26
		55	65	ACgss	10YR 5/1	Mn m			−27.5	0.165	6.2	5.8		6716	32,139	13,895	8710	356	5771	801	82	20	115	30

Holocene until Maya farmers brought agriculture and C_4 species like *Zea mays*. After allowing for bacteria fractionation that increases $\delta^{13}C$ by 2–3‰ (Webb et al., 2004), slope profiles that have only C_3 carbon isotopic signatures must reflect mainly C_3 species with levels of around −27‰. Enrichments of >3‰ in $\delta^{13}C$ in the SOM of the ancient rooting zones probably represent C_4 vegetation signatures and may indicate inputs from ancient maize fields, especially when the C_4 signatures align with dating and other lines of proxy evidence. A profile with 0–3‰ in $\delta^{13}C$ increase reflects forest or other C_3 species, naturally or by Maya land managers (Balzotti et al., 2013). These slopes may reflect the entire Holocene or may have been eroded and reflect only the soil formation in the reforestation period. Slopes that reflect C_4 species in their profiles with values as high as −12‰ likely indicate *Zea mays* or other C_4 species. Bulges of C_4 signatures in profiles may indicate inputs from ancient maize fields, especially if the C_4 signatures align with dating and other lines of proxy evidence. Balzotti et al. (2013) found that many slopes around the populous ancient Maya city of Tikal had largely C_3 signatures and ascribed this to Maya management of slopes in forest reserves, a finding also supported by the Late Classic composition of forests around Tikal as Lentz et al. (2014) reconstructed from pollen and wood charcoal. Beach et al. (in press) suggested that this pattern may equally indicate eroded areas, where soils only formed since reforestation after ancient Maya abandonment about 1000 BP. They tested this hypothesis by dating slopes and comparing soil age parameters and carbon isotope profiles. They found that backslopes had C_3 signatures of forest trees in most cases and had evidence for relative youth in high $CaCO_3$, high HCl reactions, low magnetic susceptibility, low metal elements, and coarser textures. Such findings indicate the slopes are young, which two of the above hypotheses can explain: the rapid slope inputs and outputs and the Maya-induced slope erosion hypotheses. Buried older footslopes with paleosols from ca. 2000 to 4000 BP, however, had lower $CaCO_3$ measured by Ca and by low or no HCl reactivity, higher magnetic susceptibility, higher heavy metals, and clay textures. Some also had evidence for C_4 signatures either in the younger deposits or the top of the buried soils (Beach et al., in press). This indicates ancient Maya erosion and deposition on at least some of these slopes. Indeed, these slopes show differential Maya soil management because some eroded slopes and buried footslopes occur adjacent to stabilized ancient Maya terraced slopes.

4. Field methods

For the present study, we chose five not previously studied slopes with multiple soil profiles and one additional footslope profile based on availability along archaeological transects for projects in the Programme for Belize Conservation Area and in private land nearby (Fig. 1). In conservation lands of the Programme for Belize, project members excavated 1 × 1 m or 1 × 2 m soil study units at crest-shoulder, backslope, footslope, and depression positions. On private lands at Grey Fox, Neundorf, and Tulix Mul, larger backhoe trenches provided our exposures. We determined geomorphic position and slope gradient and studied each exposure side characterizing soil colors (moist), manual texture, soil structure, HCl reaction, magnetic susceptibility, and horizons, which we revised with laboratory-based observations and analyses. We measured magnetic susceptibility of soil horizons (Dalan, 2006) in the field by placing an SM20 magnetic susceptibility meter (at a resolution of 10^{-3} SI units) flat against the soil profile and collecting measurements at 5- or 10-cm increments down the profile.

After in situ data characterization, team members collected soil samples of ca. 500 g for further analyses from all horizons and sampled some deeper horizons. They sieved soil samples in the field with 6 mm mesh and removed and recorded any artifacts from the profiles for archaeological identification. Team members identified tree species on four of the slopes to compare tree species with archaeological features and soil formation.

4.1. Laboratory methods

After shipment to the University of Texas, Austin Soils and Geoarchaeology Lab, staff members logged and processed samples. They air-dried, then disaggregated and powdered samples using mortar and pestle. They also used a Jones-style stainless steel microsplitter to generate subsamples for geochemical analysis at the Cornell Nutrient Analysis Laboratory (CNAL) and for archiving.

We include eight new Accelerated Mass Spectrometry (AMS) radiocarbon ages and seven additional ages published earlier on nearby profiles. Beta Analytic ran all the new samples of organic materials and charcoal from soil layers, which they calibrated by INTCAL98 Radiocarbon Age Calibration. Table 1 lists these as conventional and calibrated ages at the 95% probability, 2 σ level (Stuiver et al., 1998).

The CNAL determined soil texture, pH, total C by loss-on-ignition (LOI), soil organic matter (SOM) %, and soil cation exchange capability (CEC) following standard USDA procedures (cf., Burt, 2004). The laboratory measured inorganic chemistry of each soil sample using weak and strong acid digestion procedures to compare findings. The weak acid digestion used Mehlich III methods to determine the concentration of easily extractable P, K, Ca, Mg, Fe, Mn, Zn, and Al in the soils (after Mehlich, 1984). Samples of 2.0 ± 0.05 g air-dried pulverized soil were extracted with 1:10 ratio Mehlich III solution for 15 min on a reciprocating mechanical shaker (200 oscillations/min) and the supernatant extracted for dilution in preparation for analysis. The soil extracts were analyzed by Inductively Coupled Plasma Atomic Emission Spectroscopy (ICP-AES) at CNAL. The lab leached the second set of soil subsamples with a strong acid (nitric-perchloric) digestion (EPA method 3051-6010), using a mixture of concentrated HNO_3 and $HClO_4$ and 0.5 g of soil in open fluorocarbon digestion vessels heated on a digestion block for 10 min at 180 °C. The CNAL used Inductively Coupled Plasma Mass Spectroscopy (ICP-MS) to determine concentrations of 26 elements simultaneously for the 51 soil samples (Tables 2–6). Of the 26 elements analyzed, one (Mo) recorded concentrations below detection and thus we do not consider in this paper. This gave us total elements such as K, Ca, and P. Phosphorous is the most useful element for assessing human inputs into soils (Schlezinger and Howes, 2000; Holliday and Gartner, 2007). From these elements, we calculated the value of (Ca + Mg) / (Al + Fe + Mn) as a proxy for soil relative age.

We also measured the $\delta^{13}C$ of the soil humin fraction through our soils as a potential proxy for vegetation change down each soil profile. Webb et al. (2004) first hypothesized that changes in $\delta^{13}C$ of the soil humin with profile depth part of humus through a soil profile could reflect the history of vegetation change in soils used in ancient Maya agriculture. Many studies have since applied this idea to suggest historical change between C_4 (maize and/or other disturbance vegetation) and C_3 (forest species) (Beach et al., 2011, in press; Burnett et al., 2012; Balzotti et al., 2013). We used only the humin fraction (the oldest, recalcitrant portion) of humus to determine $\delta^{13}C$ with isotope-ratio mass spectrometry (for procedure details, see Balzotti et al., 2013; Beach et al., in press). We ran all humin soil samples on an EA-IRMS (elemental analyzer isotope ratio mass spectrometer) in the Light Isotope lab housed in Geosciences at the University of Texas, against a series of blanks and standards (USGS24, IAEA C7, and in-house standards).

5. Results

5.1. Chawak But'o'ob catena

Chawak But'o'ob (henceforth Chawak) is the ruin of an ancient village constructed along the sloped face of the Rio Bravo Escarpment in the Late Classic (ca. 1500–1000 BP; Walling, 2005) (Fig. 3; Table 2). Previous geomorphological studies at and around this site have

investigated floodplain and wetland formation (Beach et al., 2015b) and geochemical characterization of the limestone bedrock (Brennan et al., 2013). For this soil catena we selected a slope with minimal ancient and modern human input, 200 m away from the outer margin of the main archaeological site. We encountered only a few, undiagnostic ceramic sherds in each of our excavations, unlike copious artifacts and terraces within the ancient village.

The crest-shoulder soil is on a 3° slope and is a 42-cm-deep, slightly-to-moderately alkaline Lithic Haprendolls, with O, A1, A2, AC, and Cr horizons of *sascab* (saprolitic limestone). The topsoil consists of a 1-cm-thick O horizon above a clay loam texture and organic-rich (11% SOM) A horizon that coarsens with depth from decreased clay and increased limestone sand and gravel. This soil profile has a medium value of (Ca + Mg) / (Al + Fe + Mn), ranging from 13 to 23; and Mg and Ca increase with depth as pH rises toward the limestone parent material (Table 2). The bedrock here is dolomitic limestone with an average of ~17 wt% MgO (Brennan et al., 2013). Magnetic susceptibility is low throughout, ranging from 0.02 to 0.08 10^{-3} SI units (Table 2).

The backslope soil lies on a 15° gradient and has a thin, 28-cm-deep, slightly alkaline Lithic Haprendolls, with O, A, AC, and Cr horizons. The topsoil consists of a 1-cm-thick O horizon above a clay-textured and very organic-rich (15.4% SOM) A horizon. The SOM declines in the AC horizon down to 5.5%, and clay declines as gravel and sand increase in the clay loam textured AC horizon. This profile has a similar mid-range (Ca + Mg) / (Al + Fe + Mn) at this steep site, and magnetic susceptibility is low throughout, ranging from 0.01 to 0.08 10^{-3} SI units (Table 2).

The footslope soil lies on a 1° gradient away from the influences of frequent river flooding and alluvial fan deposition. The soil profile is a 47-cm-deep, neutral-to-moderately alkaline Lithic Haprendolls with a 1-cm-thick O and four A horizons over *sascab*. The SOM decline from the surface high of 15.5% to 2.3% in the A1, A2, A3, AC, and Cr horizons, and all horizons have clay textures throughout but decline from 84% to 40% clay as limestone gravel and sand increase down the profile. Unlike the other slope zones, Fe, Al, Mn, and Zn increase at the footslope and Ca and Mg decrease relative to the upper profiles and down profile.

This catena had moderate to low (Ca + Mg) / (Al + Fe + Mn), ranging downslope from 16 to 8 to 6 (Fig. 3). Mercury and lead concentrations, which might be derived from human inputs (Cook et al., 2006), are below detection in the crest-shoulder and backslope and very low in the footslope. Phosphorous is typically low across all locations except the topsoils on the crest-shoulder and backslope locations. Below thin O horizons, the A horizons of these Ca-rich tropical forest soils are rich in SOM. The footslope has the lowest (Ca + Mg) / (Al + Fe + Mn) values and highest concentrations of metals (Fe, Al, Ti, Zn, and Mn), including elevated Pb levels in the A1 horizon, paired with lower Mg. Likely connected to the increased Fe concentrations and Fe oxidation states, the footslope has the highest magnetic susceptibility of the catena, up to an order of magnitude higher than the crest-shoulder and backslope (Table 2).

We interpret the increase of clay at the footslope to indicate greater length of weathering time and occasional input from slope wash and low energy floodwaters. The footslope is moderately depositional from both sources and thus has been developing for a longer period than the sloping soils, which may have mostly formed since the Maya period if the soil were eroded from deforestation at that time. Even though this soil formed at the base of a slope and within reach of flood deposition, it is still a Lithic Rendolls (thinner than 50 cm; Soil Survey Staff, 2006). The increase of the heavy metal concentrations likely indicates accumulation with slope movement of older soils containing heavier metals; limestone bedrock contains mainly light metals (Ca and Mg) with low concentrations of heavier elements (Brennan et al., 2013). Paralleling the metals, the footslope soil recorded much higher magnetic susceptibility than values from the crest-shoulder and backslope (a threefold increase from the crest-shoulder to the backslope in the A3 horizon of the footslope).

Beach et al. (2015b, Fig. 2) reported a contrasting footslope excavation 200 m north at the base of the main site of Chawak that revealed

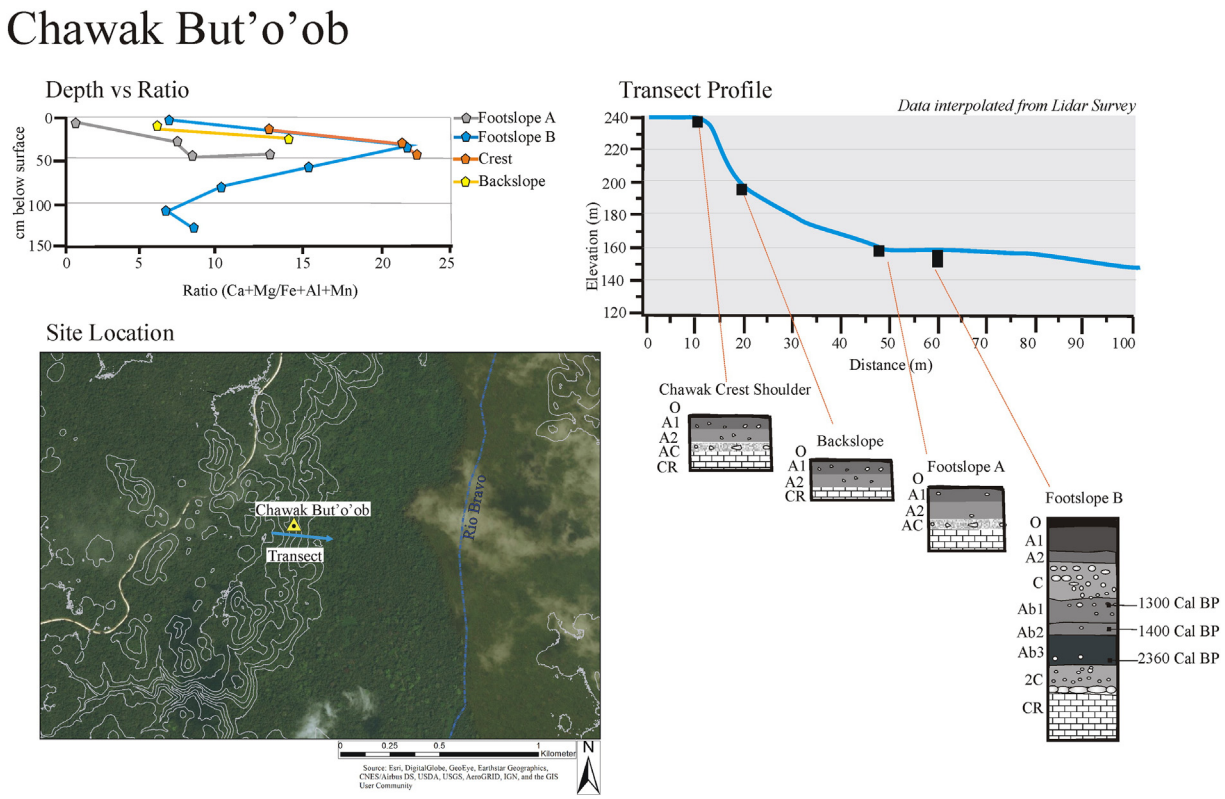

Fig. 3. Soil and elemental chemistry profiles, slope model, and map of the Chawak Catena.

a 140-cm-deep profile. This profile preserved evidence of slope deposition above a buried soil ranging from 108 to 140 cm. The upper profile has 62 cm of O, A, and C horizons lying above the Ab1, Ab2, Ab3, and 2C horizons. The Ab horizons together are a cumulic topsoil of fine textures 48 cm thick. The dating evidence for this sequence includes copious ceramics and lithics through the upper 99 cm to the top of the Ab3 horizon, and AMS dates on charred organics at 60, 80, and 108 cm with calibrated ages of 1183 to 1287, 1414 to 1544, and 2337 to 2458 BP respectively (Table 2). Magnetic susceptibility is high from the A horizon to the Ab1 horizon through enriched zone of artifacts (Table 2). We interpreted the Ab3 horizon to be the ~30-cm-thick, virgin topsoil with the sequence's high melanization, low to moderate magnetic susceptibility, and highest clay content (40%), formed over millennia at the surface, similar to the undisturbed Chawak footslope. This soil is a Cumulic Hapludolls because of the thick mollic epipedon, depth, and irregular decrease in SOM; but the lower paleosol is probably a Lithic Haprendolls (Soil Survey Staff, 2006). Similarly, the A horizon has high clay content, high melanization, a low value of (Ca + Mg) / (Al + Fe + Mn), and low amounts of high energy clasts (gravel and sand), which are 39–53% in the Classic period horizons between Ab1 down to Ab3 and 25 and 23% in the A and Ab3. We interpret the coarsening-up profile, but still with high clay contents and melanization in the Ab2 and Ab1 horizons, to indicate early soil erosion when the watershed had more melanized topsoils through the 1600 and 1300 BP dates. Above this in the C horizon the highest coarse fraction and lowest melanization may indicate the most intensive use of the watershed before the stabilization evident in the upper 25-cm A horizon. The level of (Ca + Mg) / (Al + Fe + Mn) is higher in the C horizon reflecting less sediment leaching. The stability of the A horizon may indicate the undisturbed topsoil formation since abandonment 1000 years ago or Classic Maya slope stabilization with intensive slope management. The $\delta^{13}C$ of the footslope profile here changes from −26.8‰ in the topsoil to −23.3‰ at 60 cm at the same level as the 1183 to 1287 BP age just above the Ab1 horizon before declining back to −25.8‰ in the lower Ab3 horizon age of 2337 to 2458 BP. This 3.5‰ increase in $\delta^{13}C$ indicates evidence of C_4 species in the soil humin of this buried zone.

The sedimentation rates based on ^{14}C AMS dates and sediment thicknesses (Table 2) indicate 0.37 mm y^{-1}, slow accumulation from the late Preclassic to Classic (Ab3 to Ab1), which accelerate to 0.67 mm y^{-1} in the late Classic and fall to 0.46 mm y^{-1} after 1300 BP. The topsoil here is well developed with substantial clay, and several sources suggest rapid reforestation and declining sedimentation in the Postclassic that Beach et al. (in press) estimated as 2 mm y^{-1}. We have noticed, like Wright et al. (1959) earlier, that these deep-soil slopes have larger trees and greater biodiversity.

5.2. La Milpa catena

La Milpa (Fig. 1) is a large ancient Maya urban settlement occupied between the Late Preclassic (ca. 2400–1700 BP) and Terminal Classic (ca. 1100–1000 BP) periods. The ruins lie at 190 masl on an elevated karst ridge in the La Lucha uplands. The catena runs along a 15° slope next to La Milpa Structure 3, built in the Late Preclassic and continuously modified and enlarged to the end of the Late Classic (ca. 1400–1000 BP) (Trein, 2016). Artifacts are plentiful in this area, but we noticed no walls or buildings. This soil catena contrasts with the mostly natural catena of Chawak since La Milpa formed on the edge of this ancient city, covered by tropical forest for a millennium. Again, we selected a series of crest-shoulder, backslope, footslope, and depression sites for profile examination (Fig. 4).

The crest-shoulder Cumulic Hapludolls soil had a 3° gradient slope and a 105-cm-deep profile with a thick (30 cm), organic-rich topsoil built on a C horizon, which overlay an Ab horizon from 70 to 105 cm (Table 3). The A horizon was organic-rich, highly melanized (10YR 2/1), and highly fertile with high CEC and macronutrients, including the highest levels of P recorded in this study (Table 2). Fine soil textures decreased through the A2, AC, and C horizons along with declining SOM and melanization (10YR 5/2 in the C Horizon). The (Ca + Mg) / (Al + Fe + Mn) values here are higher in the upper soil but decreases in the Ab horizon, which also has increased melanization (10YR 3/2), SOM, magnetic susceptibility, and greater clay content. These soil formation characteristics suggest that the Ab formed over longer time than the upper soil profile. Magnetic susceptibility is low throughout, with a slight uptick in the Ab horizon (Table 3).

After conducting our soil survey, we discovered that the crest-shoulder site is behind an ancient agricultural terrace. Based on ceramics, the terrace is probably Late Classic, the fill above the buried soil is Late Classic, and the Ab horizon dates to sometime earlier than the terrace and fill. The high (Ca + Mg) / (Al + Fe + Mn) values suggest that a source of less-leached soil buried the Ab horizon. A nearby agricultural terrace had a similarly buried soil with a slight increase in $\delta^{13}C$, and its Ab horizon dated to the Middle to Late Classic and the terrace to the Late Classic (Beach et al., 2002). The present study's soil profile, deep for a crest-shoulder site, had a C isotope profile that changed from −28.9‰ in the topsoil to −22.9‰ at 40 cm, which declined back to −28.9‰ in the C horizon at 60 cm before rising to −22.9‰ in the Ab horizon at 80 cm. Several sources (Webb et al., 2004; Beach et al., 2011, in press; Burnett et al., 2012; Balzotti et al., 2013) have taken an increase above 4‰ (6‰ here) in $\delta^{13}C$ to be a significant indicator of C_4 species input into SOM, which may indicate either maize agriculture in an infield or maize preparation. The double peak may also indicate two periods of C_4 species inputs separated by only C_3 through the C and upper A horizons. Perhaps this indicates C_4 inputs before and after the Late Classic terrace building. The whole soil profile had elevated P, and the Ab horizon had the second-highest level of K; both are important macronutrients.

The backslope and footslope sites were Lithic Haprendolls soils 10–35 cm deep formed over bedrock (Fig. 4). These thin soils were loamy, granular, very dark brown (10YR 2/1) A horizons over limestone and had low to moderate (Ca + Mg) / (Al + Fe + Mn) values, which may indicate more long-term soil persistence on the backslope and more deposition on the footslope. Interestingly, Zn, Fe, Al, and magnetic susceptibility were much higher in these areas than on the crest-shoulder. The footslope is only a few centimeters deeper than the backslope, where the slope break should preserve more deposition. Soil P levels peaked in the footslope, though the whole catena had elevated soil P, probably as an artifact of the history of intensive human modification here on the edge of this ancient city.

The depression site was next to a Late Classic plaza at the base of the slope. Cohune Palms (*Attalea cohune*) dominate the vegetation at this site, and SOM % is high throughout (5.5 to 6.7% to the 120-cm depth except for a coarse-textured C horizon). This Cumulic Hapludolls soil was over 100 cm deep at this site with a dark reddish grey and black (2.5YR 3/1), organic rich, loamy, granular A horizon lying above a gravelly, lower organic, clay loam Cg horizon. The Cg horizon lay above and mixed with a charcoal-, organic-, and artifact-rich Ab horizon from 50 to 85 cm (Fig. 4). The profile is the reverse of a normal profile because there are coarser textures in the upper horizons and high (Ca + Mg) / (Al + Fe + Mn) values recorded, whereas the Ab horizons appear older, based on clay textures and evidence of more leaching indicated by low (Ca + Mg) / (Al + Fe + Mn) values and the highest levels of Al, Fe, Mn, Zn, and K at the site. Likewise, magnetic susceptibility reached its peak in the Ab, reflecting metal enrichment (Hanesch and Scholger, 2002). This probably means that the upper 40–60 cm is a younger deposit from upslope erosion or ancient construction. Ceramic evidence suggested that the fill above the Ab horizon is likely Late Classic and that the clay is an earlier mixed deposit, based on our recovery of mixed-aged ceramics from the soil. This deep profile had a C isotope profile that changed from −27.3‰ in the topsoil to −24.4‰ at 80 cm, before declining back to −26.2‰ near the bottom of the profile at 90 cm. Several sources (Webb et al., 2004; Burnett et al., 2012;

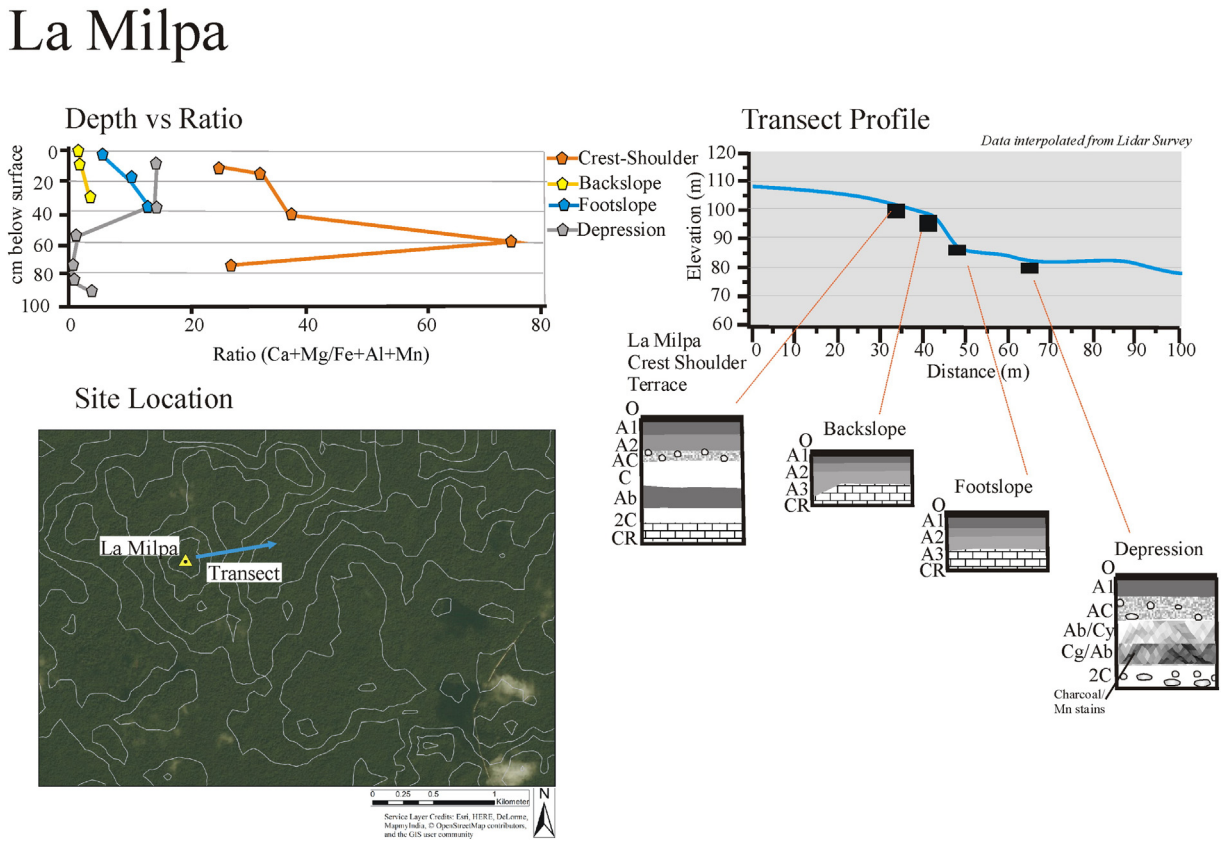

Fig. 4. Soil and elemental chemistry profiles, slope model, and map of the La Milpa Catena.

Balzotti et al., 2013) have taken the increase of nearly 3‰ in $\delta^{13}C$ herein as an equivocal indicator of C_4 species input into SOM. Thus, the crest-shoulder soil and the depression soil had buried soils and increased $\delta^{13}C$ in the profiles through the buried soils, but the crest-shoulder soil has lower amounts of clay, lower quantities of all metals, much lower (Ca + Mg) / (Al + Fe + Mn) values, and much lower magnetic susceptibility.

5.3. Grey Fox catena

Grey Fox is an ancient Maya site situated on a north-facing bluff above the Blue Creek/Rio Azul and the large Los Alacranes Bajo (*polje*) to the west (Fig. 5). The site includes large elevated plazas flanked by pyramids and multi-roomed structures. The overall form of the major architecture now exposed at the surface is typical of the Late Classic period (ca. 1400–1150 BP CE), but we lack formal excavations thus far. Smaller-scale residential structures radiate outward from the site center to an undetermined distance, giving the overall impression of a landscape that was occupied for at least several centuries and likely experienced significant ancient forest removal for urbanization and cultivation. Currently, this catena remains mantled in old growth tropical forest, though modern agriculture is encroaching from the south and west.

We opened backhoe trenches in two contexts. Operation (Op.) GF01A was in a small karst sink (*pocket bajo* between karst ridges) 600 m south of the site center (Fig. 5). Operations GF01B and 1C exposed a long, complex slope from the ridgetop of the Grey Fox site center to the floodplain of the Rio Azul. The current channel of the Rio Azul forms the Belize-Mexico border about 20 m to the north of the slope base where it has incised about 5–7 m into the floodplain (Fig. 1).

Operation GF01A was a 1 × 2.5 m trench in a small depression mantled in forest dominated by Escoba Palm (*Crysophila argentea*). Topography is locally flat to undulating, with irregular-spaced gilgai. The 2.2-m-deep backhoe trench exposed a Vertisol with a well-structured black, organic clay (85 +% clay) A horizon some 30–40 cm thick that grades irregularly into the underlying complex ACss horizon (Fig. 5; Table 4). The ACss is vertically interfingered with the overlying A in places and greatly interwoven with the underlying Cgss1 and Cgss2 horizons. In many places these horizons are indistinguishable because they blend together. Slickensides and parallelepipeds are well developed throughout the ACss and Cgss1 horizons as are vertical thrust cones extending from about 180 to 30 cm below the surface. Argilloturbation within the soil is generated by the extreme seasonality of precipitation, though uneven pressure loading during aggradation may also contribute to subsurface movement of hydrated clay within this closed basin (cf. Paton et al., 1995). Redox features including mottling, Mn nodules, and gleization increase with depth in the Cgss1 and Cgss2 horizons. The C2 horizon is the local parent material of saprolitic limestone. The level of (Ca + Mg) / (Al + Fe + Mn) was very low in all horizons except the C2 horizon, where this value rose abruptly because of coarse limestone fragments and long-term leaching to the seasonal water table. Magnetic susceptibility ranged from 0.04 to 0.15 10^{-3} SI units (Table 2).

We used three trenches to analyze the catena from the escarpment of Grey Fox into the floodplain. One hand-dug pit (Op. GF01D) exposed a backslope profile a short distance upslope from GF01C, which cut into the footslope of the long, complex slope descending down from the Grey Fox site. Operation GF01B was on the floodplain of the Rio Azul 6 m north of GF01C. The backslope profile exposed the northern flank of the Grey Fox site settlement area, where the 14° slope gradient descends into the floodplain/bajo of the Rio Azul. The soil is a thin Haprendolls with a black, clay loam A horizon averaging about 15 cm thick grading downward into a dark brown, clay loam AC horizon ranging from 5 to 30 cm in thickness over an irregular surface of weathering hard limestone. The soil profile has copious ceramics and consists of 25 to 50% angular limestone cobbles and gravel.

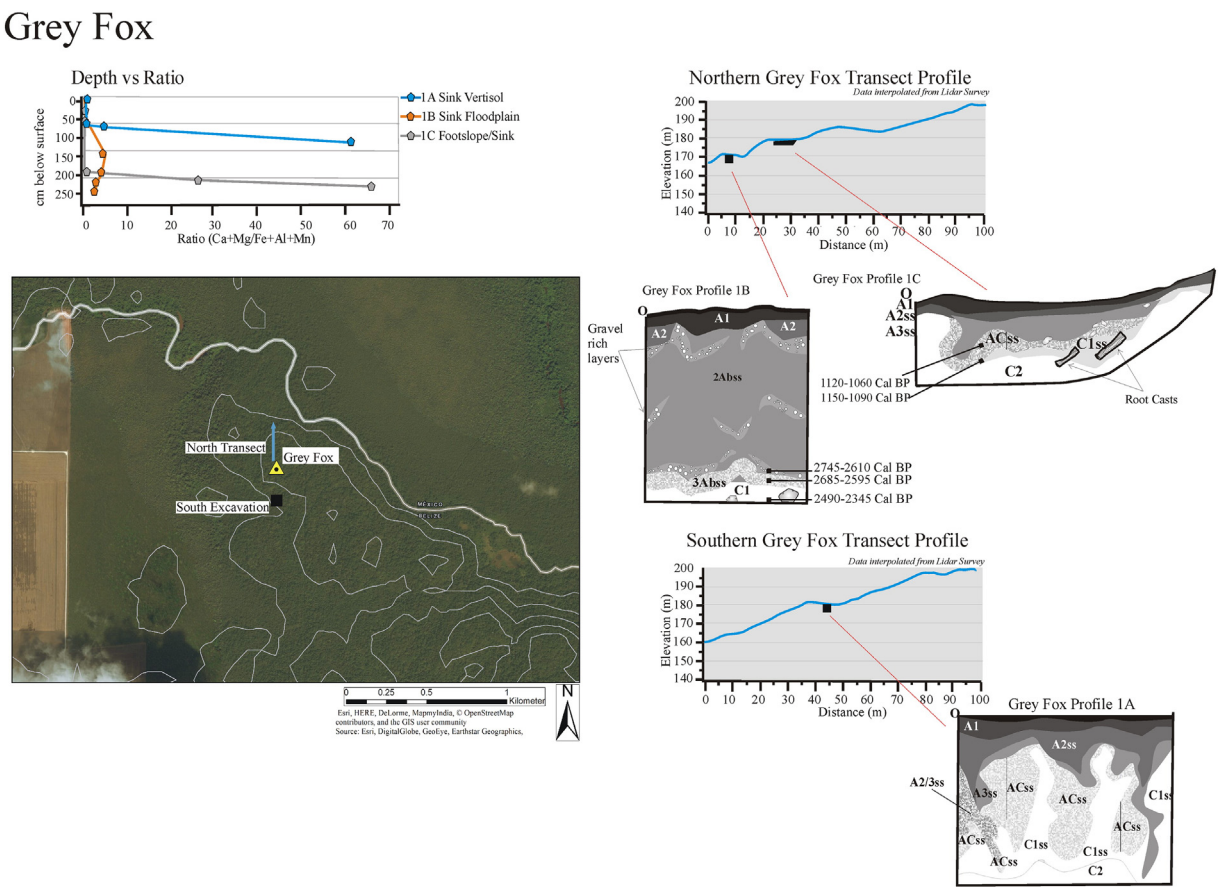

Fig. 5. Soil and elemental chemistry profiles, slope model, and map of the Grey Fox Catena.

Operation GF01C exposed a 1 × 7 m profile of the lower footslope on the northern flank of the Grey Fox site settlement area on the edge of the Rio Azul floodplain (Fig. 5). The slope gradient here ranged from 8° to 3° from south to north, with the gradual slope of a karst depression rather than a fluvial terrace edge. Riparian forest dominated this location. The upslope end of the trench exposed a shallow Haprendolls similar to GF01D; the middle portion of the trench exposed a *Vertirendolls* (described below); and the northern end of the trench penetrated a true Vertisol (Table 4). The Vertirendolls in the mid-section of the trench includes a cumulic A horizon about 80 cm thick on average. Within the A, granular structure gives way downward into a weakly developed prismatic structure as slickensides and parallelpipeds become increasingly well developed. Clay content in the A horizon is 87%, which decreases to 46% in the C horizon with increasing limestone gravel with depth. The underlying C is saprolitic limestone. Below the cumulic A horizon, an ACss horizon lies on top of the C horizon that changes significantly in terms of the (Ca + Mg) / (Al + Fe + Mn) level from ca. 0.6 to 35 and 63. Magnetic susceptibility is low, with a range of 0.01 to 0.09 10^{-3} SI units (Table 2).

Charcoal fragments within the ACss horizon at 85 and 100 cm were about 1.9 and 2.4 mg respectively and yielded calibrated radiocarbon ages of 1060 to 935 and 1170 to 960 BP respectively (Fig. 5). These dates fall within the Maya Late Classic period and suggest a sustained period of footslope aggradation during the presumed peak occupancy at Grey Fox when the slopes above were likely in some form of urban cultivation. At the lower end of the trench, where the soil deepens and grades into the floodplain, argilloturbation is significantly more pronounced in the form of a large thrust cone.

Operation GF01B, 6 m north of the north end of Op. GF01C, exposed a 1 × 3 m profile of the fluviokarst floodplain of the Rio Azul (Fig. 5). The current channel of the Rio Azul lies 15 m north of Op. GF01B and is entrenched about 2 m in its floodplain. Cohune Palms (*Attalea cohune*) dominate the vegetation, but *Tintal* (*Haematoxylum campechianu)* or seasonal swamp forest dominates closer to the river channel. The soil exposed in the excavation is a highly organic (13 to 4.5% SOM over 230 cm) Vertic Cumulic Hapludolls developed in aggrading clay-dominated sediments. The A horizon includes two components, a black (10YR 2/1) organic clay A1 and a dark reddish grey (2.5YR 3/1) A2 that is confined to pockets probably created by the decomposition of Cohune Palm root boles. The underlying 2Abss horizon is over 90% clay but is punctuated with irregular bands containing abundant, subrounded limestone and chert sand and gravel. These layers of larger clasts are most likely the product of low-frequency, high-energy flow events in the Rio Azul, probably tropical storms/hurricanes in this region. These storm deposits have been broken and distorted by subsequent argilloturbation in the interbedded clay. The remainder of the 2Abss horizon appears to be the product of slow aggradation such as would typify a slackwater area of the floodplain or a lower area of the seasonal wetland in which the floodplain is embedded. The underlying 3Abss is a very dark grey (5YR 3/1) organic clay with well-developed blocky structure and likely represents the soil surface around the time that the first Maya settlers began to colonize the Grey Fox area, evidenced in part by the presence of a few, highly weathered ceramic sherds found within this soil. Three radiocarbon samples of 812, 680, and 688 mg respectively from organic sediment and charcoal in the lower portions of the trench were BP 2745–2610 at 185 cm, BP 2685–2595 at 208 cm, and BP 2490–2345 at 233 cm (Fig. 5; Table 1). These sample ages are from just above, within, and just below the 3Abss horizon; their age inversion and partial overlap is likely a by-product of argilloturbation and associated vertical movement of soil and sediment. All of these ages fall within the Maya Middle Preclassic, a period that witnessed the widespread establishment of permanent

settlements across the Maya Lowlands, including nearby Chan Cahal (Beach et al., 2015c). This period also experienced the expansion of forest removal and cultivation -factors that can explain the onset of aggradation that buried this early Maya soil.

The (Ca + Mg) / (Al + Fe + Mn) levels through this profile range from ca. 0.37 in the upper profile to ca. 5.0 in the 2Abss horizon and declines back to 2.6 in the C horizon. This ratio level indicates highly leached clays throughout the profile with a bulge of less leached, coarser limestone clasts in the disturbance layer of the buried soils. The profile also has the highest levels of Si and highest levels of Na by a factor of 10 of all the soils in this study. Magnetic susceptibility and metal levels at 1B parallel the depression at 1A but are higher than at 1C, ranging in 1B from 0.05 to 0.13 10^{-3} SI units (Table 2).

5.4. Tulix Mul catena

Tulix Mul is an ancient Maya village comprised of a courtyard group surrounded by numerous house mounds, about 2 km south of Grey Fox (Fig. 6). The area lies on the last high point on the edge of the Alacranes Bajo, a large polje depression. Archaeological investigations at Tulix Mul have revealed that the area was occupied from 2000 to 1000 years ago (the Late Preclassic through the Terminal Classic) (Hammond, 2016).

We chose our catena slope, about 250 m north of Tulix Mul (Fig. 6), because it had a moderate gradient with no evidence of modern or ancient anthropogenic features. The catena lies between two karst hilltops with ancient occupations. The karst hilltops rise to about 110 masl, and the slope runs between these and descends from ca. 85 masl to ca. 70 masl. Our profiles here came from a backhoe trench in 2012 just two years after clearance of old-growth forest, which farmers planted to tropical C_4 grass pastures. The trench was 1.5 m wide by 1–2 m deep along a slope from its crest-shoulder to footslope and into a karst depression. The slope gradient changed from 2° at the crest-shoulder to 6.5- 7° from the shoulder to backslope in its upper 23 m, which decreased to 3–3.5° gradient from 23 to 62 m and 2° from 62 to 76 m. Beyond 100 m, the slope entered the karst depression where we backhoed a separate unit, finding a similar Vertisol as in Grey Fox 1A.

Based on mapping the profile faces, the sequence indicated a wavy pattern of deep A horizons that ranged from 45 to 70 cm thick in 2-m-wide zones interspersed with shallow A horizons that ranged from 24 to 43 cm deep in 1–2-m wide zones (Fig. 6; Table 5). This subsoil pattern had no surface expression of field undulations. We mapped and described soils over the entire reach and focused on a shoulder position with the shallower A horizon at 1 m and on a backslope and a footslope at 38 and 75 m with the deeper A horizons.

The crest-shoulder site lay above the slope with its undulating stratigraphy, and the shoulder slope had deep A horizons at 3, 7, and 10 m in the 75-m-long trench. We characterized the crest-shoulder slope at the 1-m, thinner A horizon zone. The overall A horizon thickness for this Hapludolls soil is still 30 cm with the lower wavy boundary of the Ap at 12 cm over the A2 horizon. The soil profile had clay texture throughout, with 44 to 61% clay and 21 to 44.2% sand. The SOM decreased from 12 to 3.6% through the A1 and A2 horizons, dropping to 2.3 and 4% in the layers below. We differentiated the A2 from the A1 horizons by perceptibly grayer 10YR 2/1 colors, a change from more granular to more subangular blocky structure, and more gravel (50% chert). An AC horizon with wavy upper and lower boundaries ran from 30 to 50 cm and was a mix of the dark A horizon and pale saprolitic limestone parent material. This horizon had 50–75% gravel to cobble of mixed chert and limestone. The C horizon was gravelly clay with yellow mottles from 50 to 70 cm, which lies above a Cg, gravelly clay soil with black and dark red Mn and Fe nodules from 70 to 85 cm. We did not sample and analyze the nodules here, but elemental analysis without the nodules indicated very low Mn (14 mg kg^{-1}) and Fe (2899 mg kg^{-1}) compared with the next profile down the slope, perhaps indicative of Mn and Fe removal from the soil matrix and concentration in the nodules.

Our shoulder slope description came from the 10-m point of the trench with a 7° slope. Although no samples came from this zone, the A horizon was 61 cm thick over a thin AC horizon to 65 cm and a C horizon to 82 cm. The profile had similar colors, textures, HCl reaction, and structures as the crest-shoulder above; but the A horizon was twice as thick and had no Fe or Mn nodules, perhaps reflecting decreased redox at this more sloping position.

The backslope, Cumulic Haplustolls at 38 m distance in the trench, was similar to the 10 m profile, with another thick A horizon, this time all the way to bedrock (Fig. 6; Table 5). The soil profile had clay texture throughout, with 44.9 to 62.1% clay and 15.9 to 34.4% sand. The

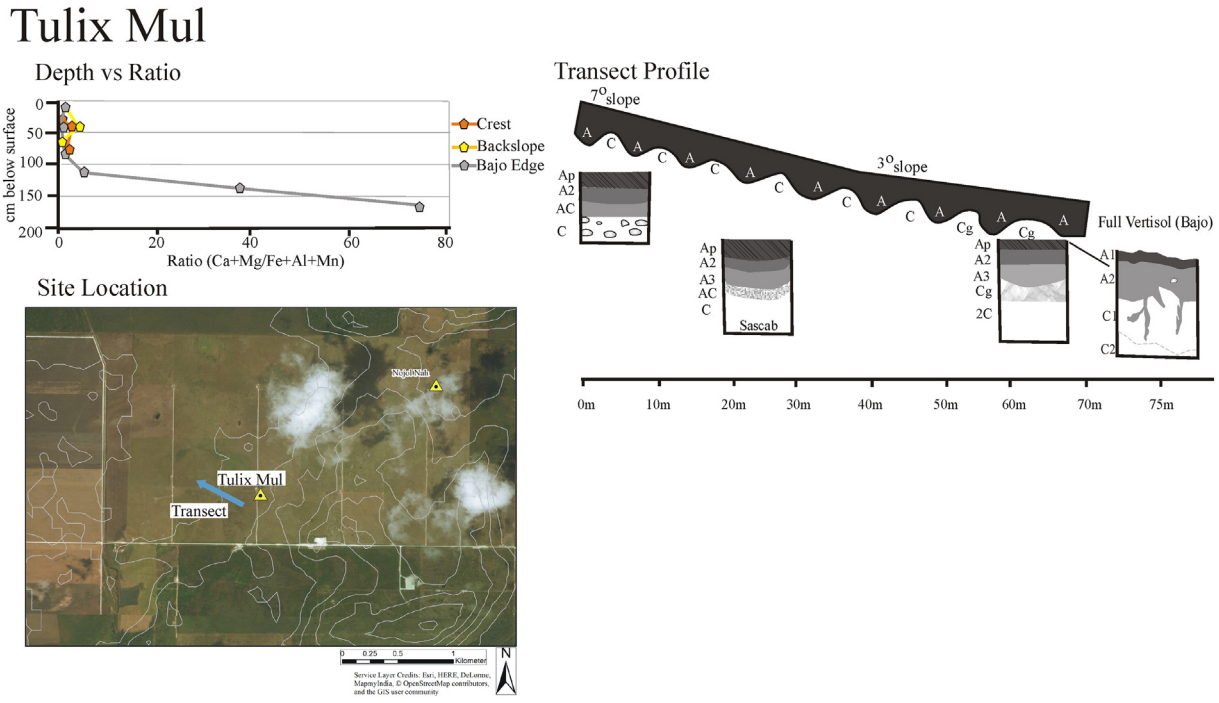

Fig. 6. Soil and elemental chemistry profiles, slope model, and map of the Tulix Mul Catena.

overall A horizon thickness was 65 cm in total with wavy boundaries between the A1, A2, A3, and AC horizons at 30, 40, and 65 cm respectively. The SOM decreased from 10.1 to 3.9% through the A1 to AC horizons. We again differentiated the A horizons by grayer 10YR 2/1 colors, a change from more granular to more subangular blocky structure and more gravel and cobble (50% chert). An AC horizon with wavy upper and lower boundaries ran from 65 to 75 cm and was a mix of the 10YR 3/1 from the A horizons and pale limestone cobble and clay. The AC horizon again had 50–75% gravel to cobble of mixed chert and limestone. We recorded a small amount of black and dark red Mn and Fe masses on surfaces but no nodules, and Mn and Fe did not decline through these horizons as they had at the crest-shoulder site. The (Ca + Mg) / (Al + Fe + Mn) values through this profile were the lowest of any of the crest-shoulder and backslopes, ranging from 0.6 to 3.2.

The Vertic Hapludolls footslope at 75 m distance lay on the edge of the karst depression at a gradient of 2°. As the slope decreased from 3.5° to 2° from 67 to 72 m distance in the trench, the rolling strata of thicker and thinner A horizons transitioned to diagonally distorted A and Css horizons as a result of Vertisol formation (Fig. 6). Beach et al. (2015c) described similar soils elsewhere in this region on older surfaces in regions with strongly seasonal wetting and drying. This soil profile had clay texture through the upper three horizons to a depth of 75 cm, with ca. 60% clay and 16% sand. The overall A horizon thickness is 50 cm with an Ap boundary at 20 cm over the A2 horizon. The SOM decreases from 9.8 to 6.7% through the Ap and A2 horizons, dropping to 5.6% in the A/Cg, and from 3.3 to 1.1% in the C horizons below. We differentiated the A2 from the Ap horizons by the plow layer's extent in this very dark brown 10YR 2/1 and 2/2 zone. The A/Cgss horizon is an argilloturbated mix of A horizon material with the underlying grey reduced clay and wavy upper and lower boundaries from 50 to 75 cm. The colors here were a mix of the 10YR 2/1 A horizon, gleyed Cg (Gley 1 4/1), and had orange mottles (Table 5). These horizons had a 25–50% mix of limestone and chert gravel and cobble. From 75 to 125 cm the C horizon is a gravelly clay loam with a matrix of orange colors and with ca. 50% gravel and cobble. Here, clay drops by 22% from above into the C horizon. Below 125 cm in the 2C horizon, there is a wavy, gradual transition from white to orange, silt loam and dominantly silt texture (63.6 and 69.5% silt) with only ca. 6% clay. Here, Ca and Mg rise by an order of magnitude, and S rises by 4 times in the zone of calcite and gypsum silt-sized crystals. Sodium, Cl, and Sr also rise through this zone. The rise of Mg indicates a large dolomitic component that Brennan et al. (2013) recognized in this region. This zone is the first in the sequence with HCl reaction, which was mild because of the dolomite and some gypsum in these carbonate silts. The footslope's 2C horizon may be a groundwater precipitate or a buried dune from much drier Pleistocene periods such as the Younger Dryas. Some scholars have noted gypsum-rich quartz dunes in similar environments across this bajo about 50 km southeast (Dunning et al., 2017).

We also ran $\delta^{13}C$ profiles for sampled soil profiles at the 10, 16, 64, and 75 m points on the trench. There was no significant change in carbon isotopes along the entire catena from the surface A horizons through depths of 145 cm and the entire range was <3‰, from −27.1 to −24.3‰ $\delta^{13}C$. These indicate signatures close to the C_3 species that dominated the slope up to 2010 with little change over time (Table 5).

Several lines of evidence indicated relatively high leaching and soil age on these slopes. There was no HCl reaction in any of the A horizons nor even on the C horizons except on limestone fragments. All soil textures were clay except three lower horizons in the footslope. Additional evidence for eluviation was the general decline of Ca, Mg, K, P, Mg, Mn, and S downward in the profile in the crest-shoulder, shoulder, and backslope, though Al and Fe did not change consistently down profile. Thus, the value of (Ca + Mg) / (Al + Fe + Mn) was generally low, increasing through the middle of the soil profile at the crest and backslopes and increasing dramatically into the carbonate parent material at the footslope. Also, Mn and Fe nodules or masses were present in all C horizons, including shoulder and backslopes (Fig. 6). It was also the only catena that had Fe and Mn masses and nodules in slope soils and where clay textures dominated all profiles. Manganese masses and nodules were common in sinks at La Milpa and DHGC 1600W, discussed below. These lines of evidence indicate greater time because they imply more leaching of carbonates, weathering of coarser to finer textures, and accumulation of allochthonous elements. This slope also has the thickest soils and lowest slope gradients, both consistent with little erosion on the slope. We suspect ancient agriculture on the slope because ancient population centers surrounded the area, but the slope gradient and ancient land practices proved insignificantly erosive. Perhaps the diminished P in these soils indicated ancient removal by farming.

5.5. DHGC 950N and 1600W catenas

These two catenas occur under primary forest with DHGC 950N having a Late Classic Maya village on its crest-shoulder and DHGC 1600W having no visible architecture nearby (Cortes-Rincon et al., 2014). We analyzed excavations at crest-shoulders, backslopes, and footslopes at both catenas and added a toeslope depression at DHGC 1600W (Fig. 7). The slope gradients at DHGC 950N ranged from 17° at the crest-shoulder to backslope, to 8° at the backslope to footslope, and 3° below this. At DHGC 1600W, slope gradients ranged from 22° from the shoulder to backslope, to 9° from the backslope to footslope, and 4° from the footslope to the depression (Table 6).

At both crest-shoulders, soil textures were loams, with 30 cm A horizons that had granular structure, 10YR 2/1 black to very dark brown colors, organic-rich, and medium HCl reactions. Both soils were shallow, 40–50 cm, with simple A over C horizon profiles. Both soils had very high concentrations of Ca, nearly 500,000 mg kg^{-1} throughout the profile at 950N and 233,000 to over 500,000 at 1600W. Both also had low concentrations of Al and Fe throughout their profiles. At 950N, Fe ranged from 1783 to 484 mg kg^{-1}, and Al ranged from 5882 to 2167 mg kg^{-1}; and at 1600W, Fe ranged from 2851 to 870 mg kg^{-1}, and Al ranged from 7592 to 2757 mg kg^{-1}. The level of (Ca + Mg) / (Al + Fe + Mn) for these crest-shoulders was high, but 1600W was lower (Fig. 7). Indeed, the major difference in these Haprendolls soils was the greater quantity of Ca through the profile at 950N, which may reflect human inputs from plaster and limestone construction near this ancient village. The relatively coarse texture (loam in a clayey soil environment), higher concentrations of Ca, and low Fe and Al at 950N may indicate relative youth because these numbers reflect the bedrock geochemistry rather than cumulative gains from aeolian deposition, which is rich in Fe and Al.

The backslope gradients at 950N changed from 17° to 8° and at 1600W changed from 22° to 9°. The A horizons at the backslopes are thick at >30 cm and had organic-rich, granular structure, 10YR 2/1, black to very dark brown colors, and medium HCl reactions. These soils are shallow, 30–40 cm, with simple A over C horizons. Compared with the crest-shoulders, backslope soils have somewhat lower Ca (but still with relatively high amounts) and more Fe, Al, and Mg. The level of (Ca + Mg) / (Al + Fe + Mn) for these backslopes was high, but 1600W was much higher (Fig. 7). The 50,000 to 70,000 mg kg^{-1} range for Mg was the highest consistently through the profiles. If the ranges of these soils reflect the bedrock, these are dolomitic limestones; or the soil profiles may be relatively more leached of Ca than Mg on these steep slopes. The major difference in these Lithic Haprendolls soils was the greater quantity of Si through the profile at 1600W, perhaps indicating more chert input at this location.

Footslope soils at 950N and 1600W had gradients of 3° and 4° respectively. The soils were deep, 80 cm at 950N and 60 cm at 1600W, with deep, cumulic A horizons of ca. 40 cm and had organic-rich, granular-structured clays with 10YR 2/1, black to very dark brown colors, and no HCl reactions above the C horizons. The profile at 1600W had AC and C horizons below the topsoils, but 950N had Ab horizons, a buried soil sequence from 50 to 80 cm. Both footslopes had

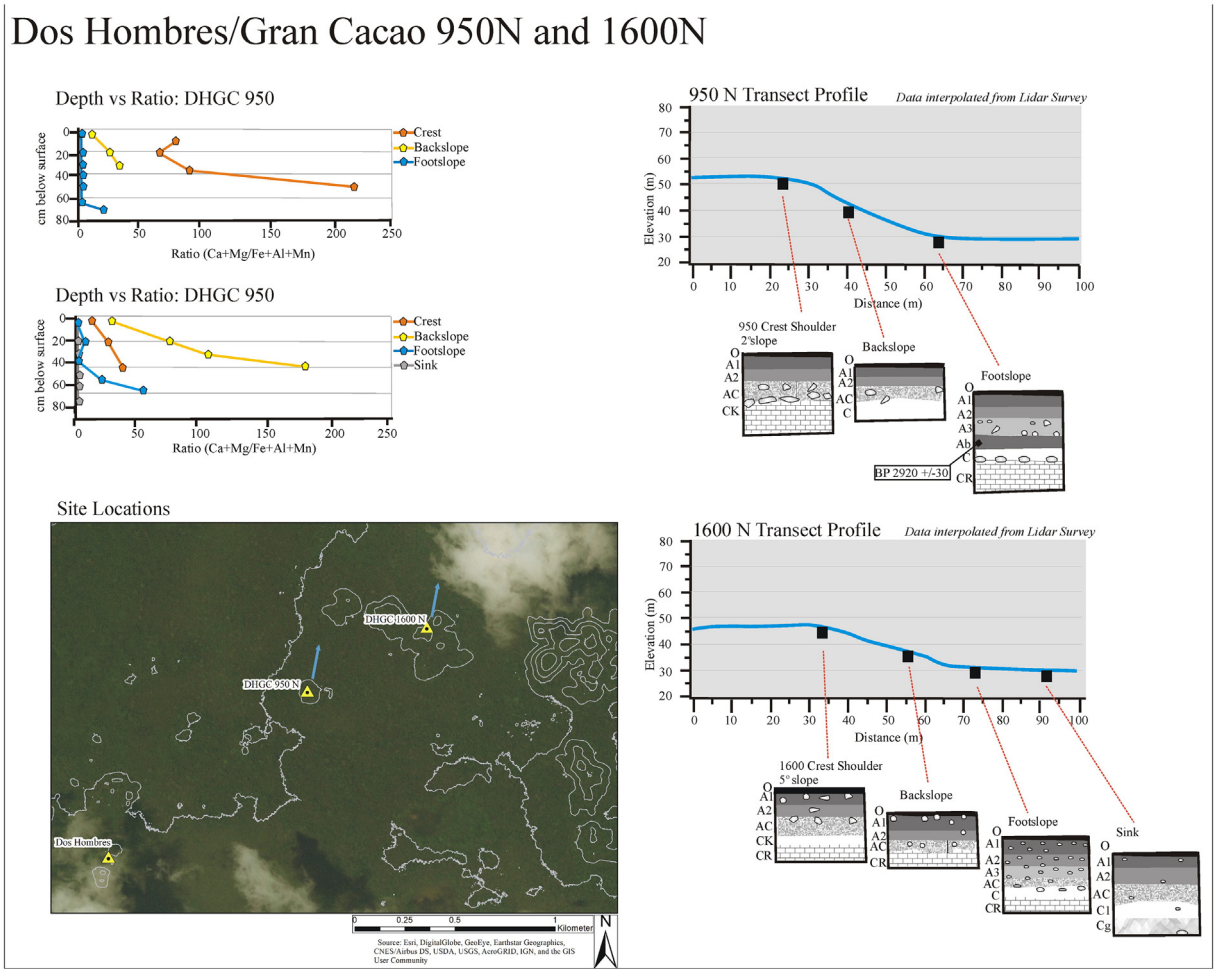

Fig. 7. Soil and elemental chemistry profiles, slope models, and map of the 950 and 1600 Catenas of the Dos Hombres to Gran Cacao Catena (DHGC) transect.

similar levels of (Ca + Mg) / (Al + Fe + Mn) with low and leached levels in the upper horizons to high Ca and Mg in the subsoil near the limestone parent material. Both soils also had low Si in the upper horizons that increased generally with depth, which probably implies more input of chert in these near bajo bedrocks.

The main differences in these two footslope soils were the buried soil, greater depth at 950N on the slope below a Maya settlement, lower Ca except in its C horizon, and higher Al, Fe, Si, and Mn. The zone of elevated Al, Fe, and Mn occurs in the sediments that bury the footslope and into the Ab horizon, but diminish while Ca and Si arise through the buried footslope C horizon, reflecting the limestone and higher chert levels near depression margins. One AMS sample of 402 mg from the 950N footslope Ab horizon at 65 cm yielded an age from organic sediment of 3165 to 2965 BP, which is an Early Preclassic age comparable to a buried footslope soil downhill from a Late Classic village under primary forest at RB73 (Beach et al., in press). Like RB73, this slope at 950N had no ancient agricultural terraces, though other nearby slopes at both locales had such terraces.

The depression soil at 1600W was on a level area in a karst sink with no HCl reaction throughout. The soil was 75 cm with a thick, cumulic A horizon of ca. 45 cm and had organic-rich, granular structure, and 10YR 2/1, black to very dark brown colors. Below the A horizon was a transitional, lighter-colored 10YR 3/1, AC horizon to 62 cm. The horizon lay below a wavy, gradual boundary to the Cr horizon at 75 cm. The Cgss had angular or wedge-like peds, Mn- and Fe-oxide streaks, with few orange mottles within the mainly grey and brown matrix, 10YR 5/3 and 5/1, clays.

This depression Vertisol had high Fe, Al, and Mn and very low Ca and Mg. This was another Cohune Palm (*Attalea cohune*) bajo as at Grey Fox and La Milpa above. Silica was high in the topsoil and C horizons, perhaps like the footslope soil above reflecting chert in the depression parent materials. The value of (Ca + Mg) / (Al + Fe + Mn) is very low, like all other sinks in this study except that near La Milpa, a large Maya city with high lime and limestone inputs. At Grey Fox, the level of (Ca + Mg) / (Al + Fe + Mn) increased only closer to limestone parent material. The 1600W profile had the lowest pH, ranging from 5.7 to 7, and from 6.3 to 5.7 below the 30 cm depth of the profile. The soil was also clay-textured throughout, ranging from 53 to 66% clay. This soil profile shows minimal sign of deposition from slope instability during the Maya period, and surveyors report no ancient buildings or terraces. The profile does, however, show a bulge of increased $\delta^{13}C$ through its AC horizons before decreasing again in the lowest horizons. The increase of 3.8‰ is significant and may indicate input of C_4 species. The fact that SOM stays high (at least 5.8% throughout the profile) may reflect, like Grey Fox 1B, the large SOM inputs from the deep-rooted and copious nut-producing Cohune Palm.

5.6. Neundorf footslope

This study includes the Neundorf footslope for comparison with the other footslopes, colluvium, and floodplain studies in this paper because it provided much better chronological control (Fig. 8). We excavated to a depth of 2 m in a trench, impeded from deeper excavation by a high-flowing artesian aquifer. The trench exposed the top of a very dark grey (GL1 3N), clay-textured, dense, granular 2Ab horizon from the bottom

of the unit at 2 to 1.7 m (Fig. 8). The 2Ab horizon had undiagnostic ceramics on its surface and 10 cm above it at 160 cm in a red (2.5YR 5/8), gravel and cobble, a charcoal radiocarbon sample of 2.1 mg was Cal BP 2145 to 1990 (Late Preclassic). Many previous excavations in this region have identified this 2Ab horizon and its lower horizons as a paleosol, often called *Eklu'um*, and multiple radiocarbon assays have always dated its surface to the Preclassic or earlier (Beach et al., 2015a). For example, 50 m away another excavation dated charred plant matter in the 2Ab horizon at a depth of 1.9 m to cal. BP 2750 to 2499 (Middle Preclassic) (Table 1). Our lowest date here lies in a fining-upward sequence of another buried soil, starting with the C2 horizon of the red cobble and extending upward to 150 cm and a very dark grayish brown (10YR 3/1), granular loam Ab horizon reaching up ca. 100 cm. A second AMS sample of 1 mg of charcoal from 116 cm in the Ab horizon yielded an age of cal. BP 1715 to 1565 (Early Classic period). From 100 to 50 cm, the C horizon was a brown (10YR 5/3) granular loam with 60% gravels and cobbles that transitioned to a black (10YR 2/1) granular clay A horizon in the upper 50 cm. This sequence shows the change from the low energy 2Ab paleosol to the high-energy facies in 2C, the stable A horizon formation to loamy soils in the Ab horizon, the instability again in the cobbly C horizon, and then stability at the surface horizon. The topsoil (50% clay) and paleosol (80% clay) are both clays sandwiching cobble and loamy sediments through the ancient Maya periods.

The soil profile at the Neundorf footslope had higher magnetic susceptibility in the buried Eklu'um paleosol and a sharp decrease to lower magnetic susceptibly in the coarser sediments above (C2 and Ab), with an increase to moderate magnetic susceptibility in the relatively stable topsoil above (Fig. 8). The fan had a C isotope profile that changed from −20.4‰ in the topsoil to - 24.6‰ at 120 cm, which we dated to 1715 to 1565 cal. YBP. The C isotope ratio continues to become more negative at the base of the profile. At 160 cm, which we date to 2145 to 1990 cal years BP, and the isotopic signature is −25.9‰. The Ab or Eklu'um paleosol at 200 cm itself has an isotopic signal of −27.4‰, typical of tropical forest (Fig. 8). This is the only soil profile with significantly elevated ^{13}C near the surface, and Beach et al. (2015c) hypothesized from similar patterns in nearby pastures that this was caused by C_4 tropical pasture grasses planted in the area since 1959.

6. Discussion

These seven new soil studies and synthesis of regional soil catenas have at least four sets of implications. The first is the information that they provide for the sediment cascade, especially new details of the depth and age of soil catenas and the timing and magnitude of sediment flux in this landscape A second group of implications is what geochemical variations on these slopes can tell us about slope history. Third, the low-gradient slope at Tulix Mul created different soils that were more leached and possessed vertic features that developed with greater time in this region. Fourth, all of these slope soils provide implications for tropical forest ecology.

6.1. Catena erosion and deposition: evidence for the sediment cascade

The sediment cascade in this landscape is most apparent on footslopes and fans (Fig. 9). Here, dated morphologic changes can indicate major facies changes and aggradation dated to the Maya period. For

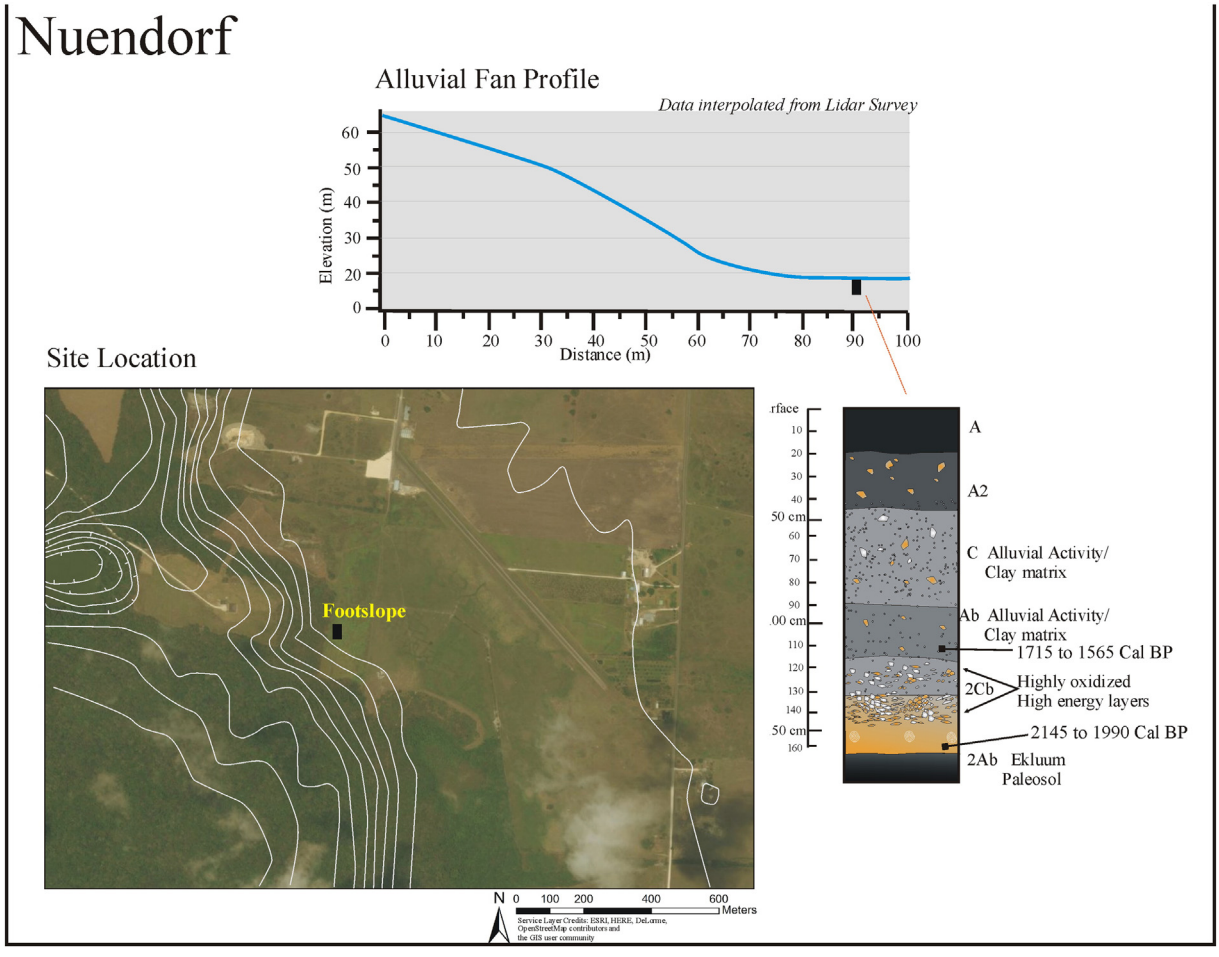

Fig. 8. Soil profile, slope model, and map of the Neundorf footslope.

example, at Neundorf, high-energy gravels and cobbles lie abruptly on an organic-rich clay paleosol, which dates through the Middle to Late Preclassic, a time of Maya expansion and early maize agriculture in this area (Beach et al., 2009). The Neundorf fan also exhibits a stable A horizon topsoil that indicates little disturbance since stabilization and subsequent abandonment 1000 years ago. Similarly, Grey Fox 1B in a floodplain depression has a disarticulated paleosol that also dates to the Middle to Late Preclassic buried by a zone of higher energy cobbles and a deep, cumulic topsoil (Fig. 5). The section of Grey Fox 1C in a footslope also has a buried horizon but here dated to the Late Classic. The footslope at 950N also has a buried soil, with one AMS date to the Maya Early Preclassic. Comparing this 950N catena downslope from an ancient Maya village with a buried footslope soil with the 1600W site with no nearby village and less evidence for burial probably implicates ancient human-induced erosion at 950N. The La Milpa footslope has a similar pattern, but we have only mixed classic artifacts on which to base the dating. We recorded two other footslopes, like 1600W above, that have little evidence of instability during ancient Maya times. The Tulix Mul footslope below a much lower gradient slope has no evidence for buried soils despite forest alteration implied by ancient villages around the slope. Likewise, the Chawak footslope, away from evidence for ancient human land use, has little evidence for instability in ancient times.

These findings are comparable with previous work. First, previous research from 200 m away and just downslope from the ancient village of Chawak displayed well-dated evidence for a facies change and instability in an alluvial fan during the Maya Classic period (Fig. 9) (Beach et al., 2015b). Second, the footslope at RB73 (Beach et al., in press) is similar to DHGC 950N in that it shows a similarly aged buried soil in a comparable setting downslope from an ancient village. Third, the Akab Muclil (Beach et al., in press) buried soil like that at La Milpa was in an ancient city and buried by slope processes downhill from urban construction. Fourth, the Crocodile Lake delta sequence (Beach et al., in press) is broadly similar to the footslopes at Neundorf and Grey Fox with sediment burial associated with the Preclassic (Fig. 9). Fifth, other footslopes and alluvial fans in the wider Maya Lowlands have similar evidence of facies changes in the Maya Late Classic period (Beach et al., 2008).

6.2. Relative ages and land uses of regional slopes from elements and isotopes

Three lines of geochemical evidence for ancient slope transformations stand out in this study. The first is the $\delta^{13}C$ signature of slope soils; the second is value of (Ca + Mg) / (Al + Fe + Mn) in this carbonate landscape; and the third is the phosphorous content in this phosphorous-limited region. The $\delta^{13}C$ signatures from SOM can reflect the history of vegetation of a soil when accounting for the 2–3‰ increase of $\delta^{13}C$ by bacterial fractionation. Using the oldest SOM fraction, soil humin, gives us a way to compare the vegetation sources of SOM on the slope over time. Almost all slope profiles in this study and others in this region and in the Yucatan (Beach et al., 2015a, 2017a) reflect the current vegetation of tropical forest, which could mean that the slopes have mainly had tropical forest vegetation or that the slopes are very young and mainly reflect vegetation and soil formation since the Maya abandonment. The only soils in this study that indicate ancient C_4 plant SOM are the Grey Fox floodplain and 1600 W depression with significant increases in $\delta^{13}C$ by 3.8‰ (up to −24.3‰) and the La Milpa crest-shoulder terrace with a significant increase in $\delta^{13}C$ of 6‰, as well as other buried horizons at Neundorf, La Milpa, and 1600W with $\delta^{13}C$ levels as high as - 24.3‰. Other studies in this region reported higher $\delta^{13}C$ from Classic period levels, especially in wetland fields (Beach et al., 2011, in press). The largest signatures of $\delta^{13}C$ levels in our study are from modern topsoils planted steadily to tropical grasses since

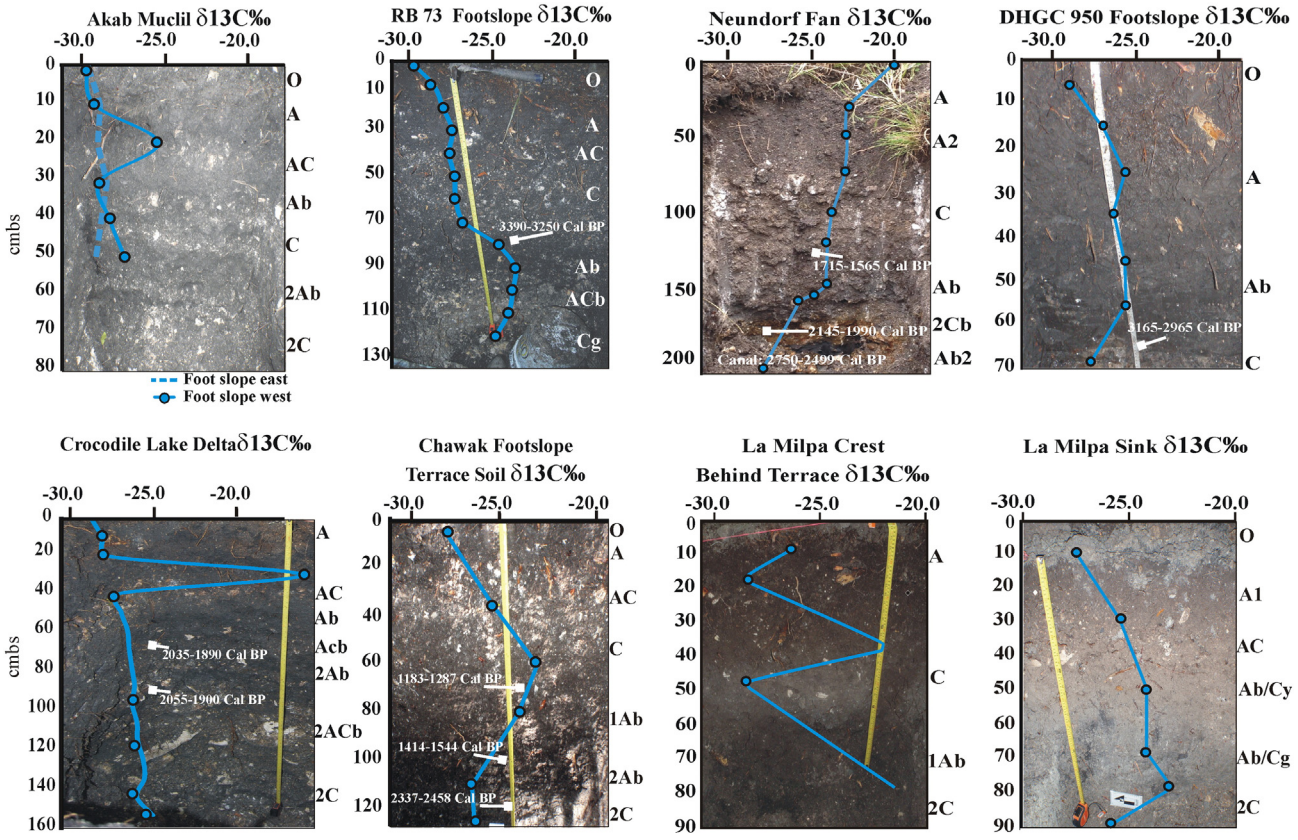

Fig. 9. Photo Mosaic of footslope and other depositional soil profiles with $\delta^{13}C$ levels plotted. We include the Akab Muclil, Chawak, RB73 footslopes, and Crocodile Lake delta from Beach et al. (in press) for comparison with soil profiles in the present study.

1959 at Neundorf and a Maya Classic agricultural terrace soil at La Milpa. Previous studies indicated more sites with elevated $\delta^{13}C$ signatures, indicating C_4 species in ancient buried soils (Beach et al., 2015a).

The level of (Ca + Mg) / (Al + Fe + Mn), the second line of geochemical evidence, may provide more insight into the relative ages of slopes and some into their vegetation histories. Slope profiles with high ratio levels indicate younger, less-weathered slopes because they reflect the carbonate parent material. In contrast, slope profiles with low ratios are relatively older, more weathered of carbonates, and indicate either in situ soils or allochthonous, weathered inputs. The Chawak soils had moderate ratios mostly ranging from ca. 6 to 23; and clearly the oldest soil horizon was the lowest at 0.84, a paleosol buried in the alluvial fan dated to BP 2337 to 2458 (Middle Preclassic). La Milpa was similar except for the Late Classic (1200 BP) crest terrace, 27–75, and the clearly older, undated buried depression soil with a ratio level of 1.1. Except for C horizons, all the Grey Fox horizons were below 1, caused by deep depression weathering at 1A and eroded old soils with leached, alluvial inputs in 1C. The one exception came from an increase to ca. 5 in the cobble zone of the 1B footslope above Middle Preclassic dates (Table 1). The Tulix Mul profiles were medium to low over the whole slope, except the depression C horizons; these must have weathered in situ on their low gradient slopes. The DHGC slopes were both moderate to high through their crests and backslope profiles and low through their footslopes and depression. We hypothesize that both of these catenas were farmed and eroded in antiquity and that the old weathered slope soils were deposited on the footslopes and depressions. The buried soil with a Middle Preclassic date (Table 1) at the footslope in 950N provides evidence for this, and perhaps the high SOM throughout the 1600W depression soil, together with its increase of $\delta^{13}C$ by 3.8‰ in the ACss horizon, indicates that it is really a topsoil from an old buried weathered backslope.

Three other lines of evidence for relative slope ages are soil textures, skeletal horizons, and Fe and Mn masses and nodules. These all show that the crest through backslope soil profiles at DHGC at 950N and 1600W, the backslopes and footslopes at La Milpa, and the Chawak crest-shoulder and backslopes are young based on their generally coarser textures, low magnetic susceptibility, and lack of Fe and Mn masses and nodules. Comparing these slopes with Grey Fox and Tulix Mul again indicates that the Grey Fox and Tulix Mul profiles are finer-grained (predominantly clays), thicker, and both have Fe and Mn nodules and masses.

Magnetic susceptibility could be an equivocal measurement for relative age of slopes. Elevated levels could be from old soils enriched in metals, anthropogenic metal and burning inputs, or bedrock variations. The highest magnetic susceptibility comes from the edge of a platform in the La Milpa sink, which also has the highest metal concentrations and intensive anthropogenic inputs. The second highest levels come from the 1600W footslope and sink and the 950N footslope, which also have high metals and lower evidence and higher evidence respectively for human-induced erosion. The third highest levels occur in the Chawak footslope and alluvial fan in similar conditions. In total, the variations in magnetic susceptibility across these catenas implicate variable anthropogenic inputs.

A clear impact with ramifications for soil ages on catenas are ancient Maya terraces. Ancient terracing is widespread and is a key soil formation factor and part of slope geomorphology in many parts of the Maya Lowlands (Beach et al., 2015a). We discovered one such terrace in these catena studies, even though our original research design was to focus on soils with little human impact (Fig. 9). Thus far, our studies have found widely different evidence for how the Maya used terraces (Beach et al., 2015a, in press) and that many terraces still function to retain soils after the one to two millennia since construction. Some soils behind terraces also preserved and augmented preexisting soils such as at La Milpa in this study. Where these terraces occur, they deepen soils and increase soil moisture, a form of niche construction that reverberates through the ecosystem. With the growth of widespread LiDAR, we can begin to quantify these impacts on the Maya tropical forest and its geomorphology (Chase et al., 2014).

Another line of evidence for past human impacts on these soils is phosphorous because this element is in generally short supply in Maya Lowlands soils. It is scarce in the limestone parent materials, such as those exposed in the C horizons in our study sites. The main sources that can enrich P in regional soils are human and aeolian, and cropping rapidly depletes P unless offset with soil amendments (Beach et al., 2015a). Two catenas stand out for higher P and lower P, La Milpa and Tulix Mul respectively. The entire slope at La Milpa, an ancient Maya city, has very high P (201–508 mg kg^{-1}), despite its skeletal soils. The entire slope at Tulix Mul, a long-lasting Maya village, has low P (49–298 mg kg^{-1}), despite its thick, organic-rich, low gradient soils.

Phosphorous has normal levels and decreases down profile at most sites such as 1600W and 950N. We note that P persists in high amounts through the soil profiles in only the Chawak alluvial fan, the La Milpa crest terrace and slopes, and the Grey Fox 1B floodplain profile exhibit (Table 4). Phosphorous remains relatively high from the Preclassic buried soil through the Classic period aggradation from runoff from the ancient village of Chawak. A similar pattern occurs at the La Milpa crest terrace, which dates to the Late Classic. In the Grey Fox 1B profile, P is high (≥281 mg kg^{-1}) in the epipedon, diminishing with depth until the lowest part of the 2Abss and 3Abss, where levels climb again to over 200 mg kg^{-1}. This pattern may indicate adequate P levels in the Middle Preclassic soils associated with a long period of landscape stability and intact forest cover, diminishing P over time in the cumulic 2Abss as source soil/sediment was increasingly derived from cultivated soil, then elevated levels again with landscape abandonment and reforestation.

6.3. The Tulix Mul catena

The Tulix Mul catena was different from the others because of its lower gradient slope along its bajo edge location, rolling stratigraphy, and its low level of (Ca + Mg) / (Al + Fe + Mn) (Fig. 6). There are at least two hypotheses to explain the rolling stratigraphy of deeper and shallower A horizons in the Tulix Mul slope profile. The first explanation is that the longitudinal profile over 68 m represents mukkara (Paton et al., 1995) caused by expansion and contraction from vertic argilloturbation producing vertic features. As with mukkara elsewhere, the Tulix Mul soils have a high clay content and moderate slopes of 2 to 7°. Most soils in this region have a high quantity of smectite clay (Tankersley et al., 2016), a 2:1 clay that would also increase the expansion and contraction necessary to produce the rolling strata of the mukkara. A second hypothesis to explain the rolling strata could be an ancient Maya land use pattern, such as field ridging or *camellones* in the same vein as contour plowing to decrease erosion from overland flow and maintain soil moisture. Evidence in keeping with ancient Maya field ridges is the copious ceramics and lithics through the soils and the nearby occupation contexts. Additionally, field ridging like this occurs in the volcanically buried Classic period village of Cerén (Sheets et al., 2012). Nevertheless, evidence for the natural explanation is the fact that the mukkara-like Vertisol features transition into other typical Vertisol features as the slope changes angle from 3.5 to 2° from the backslope to footslope. We expect that the mukkara and field ridge models would have a surface expression of gilgai or ridge microtopography, but we did not observe this. Bioturbation in the millennium since Maya abandonment and recent plowing since deforestation in 2010 could have expunged this surface, though gilgai patterns are usually still apparent after plowing. The rolling stratigraphy on this low-gradient slope is an equifinality in the absence of further evidence.

6.4. Ecological implications for the Maya Forest

The ecological implications from this study include the differences in soil profile catena positions, the degree these profile positions were altered by humans, and the association of cumulative soils with Cohune Palms. Deeper soils occurred at crests and footslopes as well as at agricultural terraces. The La Milpa crest-shoulder also happened to coincide with an agricultural terrace and elevated P even at the lowest soil level. This should impart greater nutrients to plants, and the deeper soils should hold more soil moisture for plants to last longer through the dry season. The thinnest soils occurred on backslopes, which ranged from 30 to 42 cm, except for the deeper soils at the low gradient slope at Tulix Mul. Thinner soils would have fewer nutrients and a lower soil water supply. We hypothesize that these variations should influence tree species and forest structure, and Hightower et al. (2014) showed that deeper soils of ancient agricultural terraces had taller forests with greater canopy diversity and fewer gaps.

Also, Cohune Palms were the dominant plant at three of our study sites, and these soils were deeper with greater SOM throughout their profiles. The Grey Fox sink, for example, had a remarkable depth of cumulative A horizons (over 230 cm) and high SOM content. The La Milpa and the DHGC 1600W sinks also had high SOM throughout their profiles (mostly above 5%). The deep root system of these palms may penetrate >1 m; and they provide copious large nuts, leaf, and root litter (Furley, 1975). They also have higher Si based on elevated levels at Grey Fox and DHGC 1600W, which we suggest may be caused by high phytolith inputs or preservation from the palms or to increased chert around bajo edges.

7. Conclusions

Soil catenas from the Maya tropical forest of northwestern Belize near its boundaries with Guatemala and Mexico provide an important laboratory to study resilience in biogeomorphic systems. Conserved forest in this region preserved primary forest with little human impacts for a millennium, but the forest canopy also obscures ancient Maya land uses from 3000 to 1000 years ago that ranged from intensive city- and farm-scapes to extensively managed forests. This study provides new evidence from 22 soil profiles with a range of these ancient land uses on their limestone, fluviokarst slopes. The soil profiles came from six new slopes and one new alluvial fan. Five of the slopes and one more above the alluvial fan had tropical forest vegetation for a millennium and one had been deforested only two years before our study.

Our research synthesis indicates that the region experienced general soil stability through the Holocene until human impacts started to cause instability around 3000 years ago, stability again after the Maya abandonment of these regions around BP 1000, and instability once again with recent deforestation. All the slope soil dates in the current study and most in recent studies are from the Holocene, indicating Holocene formation. A few depression soils have produced Pleistocene dates. Key lake core evidence tells us that most of the sedimentation (and erosion) in the Holocene occurred during the Maya period in the form of *Maya Clays*. Some of this evidence also tells us that soil erosion declined during the period of highest population and land use intensity in the Maya Classic period from about 1700 to 1000 BP, which indicates either resilience through conservation or another form of resilience in biogeomorphic systems, namely source exhaustion (removal of available soils).

The current study gives us insight into this question from slope catenas and footslopes; and these provide evidence for human resilience and adaptation, possible soil exhaustion, and ecosystem resilience in the return of old growth forests to soils once diminished and enhanced in antiquity. Two slopes in this study show conservation, one with a terrace on a crest slope at La Milpa that retained a thick, fertile, phosphorous-rich soil from over a millennium ago; and a second example at Tulix Mul in the midst of ancient villages indicated no soil erosion although low in phosphorous, a critical macronutrient. The Tulix Mul soil catena remained thick and organic-rich either because it was not steep enough or because ancient land managers conserved it, perhaps by forest cover because of the consistently low $\delta^{13}C$ indicative of C_3 species. There are many other conserved slopes across this region, because of the many terraced slopes here. The terrace in this study emphasizes their frequency because we had originally selected catenas in this study that did not appear to have terraces as we surveyed the forested slopes.

Many lines of evidence suggest that other slopes were likely eroded in ancient times: buried soils at footslopes and evidence for young backslope soils in little-weathered soil and thinner profiles, coarser textures, and lack of evidence for greater soil age. The most obvious example here are the footslopes and fans that show facies changes that date from the Maya period. These include several examples of well-developed buried soils with clay textures buried by sediments with coarse textures and little other evidence of soil development. The Neundorf fan, Grey Fox floodplain fan, the 950N footslope, the Chawak fan, and the La Milpa depression presented here as well as other examples reviewed here provide cases of stable soils buried during Maya periods that are now capped by well-developed topsoils formed since Maya abandonment after centuries of reforestation. Upslope from some of these footslopes and fans are also examples of sloping soils (with gradients above 15°) that have multiple characteristics of youth with their high carbonate elements, coarse textures, and thin profiles.

The sediment cascade in any landscape is complex and the number of soil slopes and storage sites we studied in this environment is only a beginning. We need more such studies to better model sediment movement and soil formation over time. Going beyond the sediment cascade will be understanding the long-term Maya impacts on the remaining Maya forest. To understand this, we need to compare these soil catenas with quantitative measures of tree species that grow on them. This may indicate several aspects of biodiversity like species diversity, canopy complexity, and canopy heights that we can correlate with the soil parameters we presented in this study. Do the preserved slopes with thicker, more fertile soils have higher biodiversity? Are forests on the more skeletal slopes from ancient erosion less biodiverse? Are the footslopes with their thicker soils and greater moisture capacity more biodiverse, or do they have taller, larger trees? We also identified three soils that had cumulic zones of organic-matter-rich soils that correlate with Cohune Palms (*Attalea cohune*), which scholars since Wright et al. (1959) have linked with uniquely organic-rich and deep soils. Beyond this correlation, our next step with the aid of high resolution LiDAR imagery and more ground studies will be to map and test soils to understand their geographic extent and ecological importance as, for example, biodiversity hotspots, niche creators, carbon sequestration zones, and other legacies of millennia of Maya civilization on soils and forests.

Acknowledgements

The following organizations deserve thanks for funding this research: The University of Texas at Austin, The C.B. Smith, Sr., Centennial Chair; Brigham Young University; grants from the National Geographic Society (CRE-7506-03, CRE-7861-05; T. Beach and S. Luzzadder-Beach PIs) and the National Science Foundation (Nos BCS-0924510, T. Beach, PI; BCS-0924501 and BCS-1550204, S. Luzzadder-Beach, PI; GEO-CNH-1114947, N. Brokaw, S. Ward, M. Cortes-Rincon, S. Luzzadder-Beach, and S. Walling; BCS-0241757, N. Dunning PI; SBR 963-1024, V. Scarborough and N. Dunning); and George Mason University's Center for Global Studies and Provost's Office. We also thank the Maya Research Program, Dr. T. Guderjan, Director; The Programme for Belize Archaeological Project, Dr. F. Valdez Jr., Director; and the Institute of Archaeology, National Institute of Culture and History, Belize, The Programme for Belize; and the communities of Blue Creek and San Felipe. We thank P. Magana, K. Cox, Esq., D., B., and M. Dyck, William Johnson, Richard

Marston, anonymous reviewers, and many graduate and undergraduate students of our institutions.

References

Adams, R.E.W., Robichaux, H.R., Valdez Jr., F., Houck, B., Mathews, R., 2004. Transformations, periodicity, and urban development in the Three Rivers region. In: Demarest, A., Rice, P., Rice, D. (Eds.), The Terminal Classic in the Maya Lowlands: Collapse. Transition and Transformation. University Press of Colorado, Boulder, CO, pp. 302–323.

Akpinar-Ferrand, E., Dunning, N., Lentz, D., Jones, J., 2012. Aguadas as water sources at Southern Maya Lowland sites. Anc. Mesoam. 23, 85–101.

Anselmetti, F.S., Hodell, D.A., Ariztegui, D., Brenner, M., Rosenmeier, M.F., 2007. Quantification of soil erosion rates related to ancient Maya deforestation. Geology 35, 915–918.

Balzotti, C.S., Webster, D.L., Murtha, T.M., Petersen, S.L., Burnett, R.L., Terry, R.E., 2013. Modelling the ancient maize agriculture potential of landforms in Tikal National Park, Guatemala. Int. J. Remote Sens. 34 (16), 5868–5891.

Bautista, F., Palacio Aponte, G., Quintana, P., Zinck, J.A., 2011. Spatial distribution and development of soils in tropical karst areas from the Peninsula of Yucatan, Mexico. Geomorphology 135, 308–321.

Beach, T., 1998. Soil catenas, tropical deforestation, and ancient and contemporary soil erosion in the Petén, Guatemala. Phys. Geogr. 19, 378–404.

Beach, T., Luzzadder-Beach, S., Dunning, N., Hageman, J., Lohse, J., 2002. Upland agriculture in the Maya Lowlands: ancient conservation in northwestern Belize. Geogr. Rev. 92 (3), 372–397.

Beach, T., Dunning, N., Luzzadder-Beach, S., Cook, D.E., Lohse, J., 2006. Impacts of the ancient Maya on soils and soil erosion in the central Maya lowlands. Catena 65, 166–178.

Beach, T., Luzzadder-Beach, S., Dunning, N., Cook, D., 2008. Human and natural impacts on fluvial and karst depressions of the Maya Lowlands. Geomorphology 101 (1/2), 308–331.

Beach, T.P., Luzzadder-Beach, S., Dunning, N.P., Jones, J.G., Lohse, J.C., Guderjan, T.H., Bozarth, S., Millspaugh, S., Bhattacharya, T., 2009. A review of human and natural changes in Maya Lowlands wetlands over the Holocene. Quat. Sci. Rev. 28, 1710–1724.

Beach, T.P., Luzzadder-Beach, S., Dunning, N.P., Terry, R., Houston, S., Garrison, T., 2011. Carbon isotopic ratios of wetland and terrace soil sequences in the Maya Lowlands of Belize and Guatemala. Catena 85, 109–118.

Beach, T., Luzzadder-Beach, S., Cook, D., Dunning, N., Kennett, D., Krause, S., Terry, R., Trein, D., Valdez, F., 2015a. Ancient Maya impacts on the Earth's surface: an Early Anthropocene analog? Quat. Sci. Rev. 124, 1–30.

Beach, T., Luzzadder-Beach, S., Krause, S., Walling, S., Dunning, N., Flood, J., Guderjan, T., Valdez, F., 2015b. 'Mayacene' floodplain and wetland formation in the Rio Bravo watershed of northwestern Belize. The Holocene 25 (10), 1612–1626.

Beach, T., Luzzadder-Beach, S., Guderjan, T., Krause, S., 2015c. The floating gardens of Chan Cahal: soils, water, and human interactions. Catena 132, 151–164.

Beach, T., Luzzadder-Beach, S., Sweetwood, R.V., Farrell, P., Mazeau, D., Terry, R.E., 2017a. Soils and agricultural carrying capacity. In: Hutson, S. (Ed.), Ancient Maya Commerce: Multidisciplinary Research at Chunchucmil. University Press of Colorado, Boulder, CO, pp. 197–219.

Beach, T., Ulmer, A., Cook, D., Brennan, M., Luzzadder-Beach, S., Doyle, C., Eshleman, S., Krause, S., Cortes-Rincon, M., Terry, R., 2017b. Geoarchaeology and tropical forest soil catenas of northwestern Belize. Quat. Int. http://dx.doi.org/10.1016/j.quaint.2017.02.031 (In Press).

Boose, E.R., Foster, D.R., Fluet, M., 1994. Hurricanes impacts to tropical and temperate forest landscapes. Ecol. Monogr. 64, 369–400.

Brennan, M.L., King, E.M., Shaw, L.C., Walling, S.L., Valdez Jr., F., 2013. Preliminary geochemical assessment of limestone resources and stone use at Maya sites in the Three Rivers Region, Belize. J. Archaeol. Sci. 40, 3178–3192.

Brewer, S.W., Rejmánek, M., Webb, M.A.H., Fine, P.V.A., 2003. Relationships of phytogeography and diversity of tropical tree species with limestone topography in southern Belize. J. Biogeogr. 30 (11), 1669–1688.

Brokaw, N.V.L., Mallory, E.P., Schulze, M., Novelo, D., Hess, S., Taylor, C., 1993. Vegetation of the Rio Bravo Conservation and Management Area, Belize. Manomet Bird Observatory, Manomet, MA.

Bundschuh, J., Alvarado Induni, G., 2007. Central America: Geology, Resources, and Hazards. Taylor & Francis, London, UK.

Burnett, R.L., Terry, R.E., Alvarez, M., Balzotti, C., Murtha, T., Webster, D., Silverstein, J., 2012. The ancient agricultural landscape of the satellite settlement of Ramonal near Tikal, Guatemala. Quat. Int. 265, 101–115.

Burt, R. (Ed.), 2004. Soil Survey Laboratory Methods Manual. Soil Survey Investigations Report No. 42. USDA-NRCS. National Soil Survey Center, Lincoln, NE.

Cabadas, H., Solleiro, V.E., Sedov, S., Pi, T., Alcala, J.R., 2010. The complex genesis of red soils in peninsula de Yucatán, Mexico: mineralogical, micromorphological and geochemical proxies. Eurasian Soil Sci. 43 (13), 1439–1457.

Cabadas-Báez, H., Solleiro-Rebolledo, E., Sedov, S., Pi, T., Gama-Castro, J., 2010. Pedosediments of karstic sinkholes in the eolianites of NE Yucatan: a record of Late Quaternary soil development, geomorphic processes, and landscape stability. Geomorphology 122, 323–337.

Chase, A.F., Chase, D.Z., Awe, J.J., Weishampel, J.F., Iannone, G., Moyes, H., Yaeger, J., Brown, M.K., 2014. The use of LiDAR in understanding the ancient Maya landscape: Caracol and Western Belize. Adv. Archaeol. Pract. 2 (3), 147–160.

Cook, D., Kovacevich, B., Beach, T., Bishop, R., 2006. Deciphering the inorganic geochemical record of ancient human activity using ICP-MS: two examples from Late Classic soil floors at Cancuen, Guatemala. J. Archaeol. Sci. 33 (5), 628–640.

Cook, D.E., Beach, T., Demarest, A.A., 2017. Slaughter and soil: a geophysical record of the late Classic Maya from Cancuen, Guatemala. J. Archaeol. Sci: Reports (In press).

Cortes-Rincon, M., Boudreaux, S., Marinkovich, E., Brennan, M.L., 2014. Household and elite labor investments at the Dos Hombres to Gran Cacao Archaeology Project. Res. Rep. Belizean Archaeol. 11, 143–153.

Coultas, C.L., Collins, M., Chase, A., 1993. The effect of ancient Maya agriculture on terraced soils of Caracol, Belize. In: Foss, J., Timpson, M.E., Morris, M.W. (Eds.), Proceedings of the First International Conference on Pedo-Archaeology. The University of Tennessee Press, Knoxville, TN, pp. 191–201.

Coultas, C.L., Collins, M., Chase, A., 1994. Some soils common to Caracol, Belize and their significance to ancient agriculture and land use. In: Chase, D., Chase, A. (Eds.), Studies in the Archaeology of Caracol, Belize. Pre-Columbian Art Research Institute Monograph 7, San Francisco, CA, pp. 21–33.

Coultas, C.L., Hsieh, Y.P., Post, T.J., 1997. A Toposequence of Soils in Northern Belize, Central America. 56. Soil and Crop Science Society of Florida, pp. 117–124.

Dalan, R.A., 2006. A geophysical approach to buried site detection using down-hole susceptibility and soil magnetic techniques. Archaeol. Prospect. 13, 182–206.

Deevey, E.S., Rice, D.S., Rice, P.M., Vaughan, H.H., Brenner, M., Flannery, M.S., 1979. Mayan urbanism: impact on a tropical karst environment. Science 206, 298–306.

Douglas, P.M.J., Pagani, M., Canuto, M.A., Brenner, M., Hodell, D.A., Eglinton, T.I., Curtis, J.H., 2015. Drought, agricultural adaptation, and sociopolitical collapse in the Maya Lowlands. Proceedings of the National Academy of Sciences. 112, pp. 5607–5612.

Dunning, N.P., Beach, T., 2000. Stability and instability in Pre-Hispanic Maya landscapes. In: Lentz, D. (Ed.), Imperfect Balance: Landscape Transformations in the Pre-Columbian Americas. Columbia University Press, New York, NY, pp. 179–202.

Dunning, N.P., Jones, J.G., Beach, T., Luzzadder-Beach, S., 2003. Physiography, habitats, and landscapes of the Three Rivers Region. In: Scarborough, V., Valdez, F., Dunning, N.P. (Eds.), Heterarchy, Political Economy and the Ancient Maya: The Three Rivers Region of the East-Central Yucatan Peninsula. University of Arizona Press, Tucson, AZ, pp. 14–24.

Dunning, N.P., Beach, T., Luzzadder-Beach, S., Jones, J.G., 2009. Creating a stable landscape: soil conservation among the ancient Maya. In: Fisher, C.T., Hill, B., Feinman, G. (Eds.), The Archaeology of Environmental Change: Socionatural Legacies of Degradation and Resilience. University of Arizona Press, Tucson, AZ, pp. 85–105.

Dunning, N., Beach, T., Luzzadder-Beach, S., 2012. Kax and Kol: collapse and resilience in Lowland Maya civilization. Proc. Natl. Acad. Sci. 109, 3652–3657.

Dunning, N., McCane, C., Swinney, T., Purtill, M., Sparks, J., Mann, A., McCool, J.-P., Ivenso, C., 2015a. Geoarchaeological investigations in Mesoamerica move into the 21st century: a review. Geoarchaeology 30, 167–199.

Dunning, N.P., Griffin, R., Jones, J.G., Terry, R., Larsen, Z., Carr, C., Lentz, D.L., 2015b. Life on the edge: Tikal in a bajo landscape. In: Dunning, N.P., Scarborough, V. (Eds.), Tikal: Paleoecology of an Ancient Maya City. Cambridge University Press, Cambridge, UK, pp. 95–123.

Dunning, N., Griffin, R., Sever, T., Saturno, W., Jones, J., 2017. The nature and origin of linear features in the Bajo de Azúcar, Guatemala: implications for ancient Maya adaptations to a changing environment. Geoarchaeology 32, 107–129.

Escobar, J., Hodell, D.A., Brenner, M., Curtis, J.H., Gilli, A., Mueller, A.D., Anselmetti, F.S., Ariztegui, D., Grzesik, D.A., Pérez, L., Schwalb, A., Guilderson, T.P., 2012. A ~43-ka record of paleoenvironmental change in the Central American lowlands inferred from stable isotopes of lacustrine ostracods. Quat. Sci. Rev. 37:92–104 ISSN 0277-3791. http://dx.doi.org/10.1016/j.quascirev.2012.01.020.

Furley, P.A., 1975. The significance of the cohune palm, Orbignya cohune (Mart) Dahlgren, on the nature and in the development of the soil profile. Biotropica 7 (1), 32–36.

Furley, P., 1987. Impact of forest clearance on the soils of tropical cone karst. Earth Surf. Process. Landf. 12, 523–529.

Furley, P.A., Newey, W.W., 1979. Variations in plant communities with topography over tropical limestone soils. J. Biogeogr. 6 (1), 1–15.

Hammond, G., 2016. Water, Stone and Soil: A preliminary investigation into the location of selected sites in far northwest Belize in relation to critical natural resources. In: Guderjan, T. (Ed.), The Ancient Maya City of Blue Creek. Wealth, social Organization and Ritual. BAR Press, Oxford, UK, pp. 17–29.

Hammond, N., Tourtellot, G., Donaghey, S., Clarke, A., 1998. No slow dusk: Maya urban development and decline at La Milpa, Belize. Antiquity 72, 831–837.

Hanesch, M., Scholger, R., 2002. Mapping of heavy metal loadings in soils by means of magnetic susceptibility measurements. Environ. Geol. 42, 857–870.

Hightower, J.N., Butterfield, A.C., Weishampel, J.F., 2014. Quantifying ancient Maya land use legacy effects on contemporary rainforest canopy structure. Remote Sens. 6, 10716–10732.

Hodell, D.A., Anselmetti, F.S., Ariztegui, D., Brenner, M., Curtis, J.H., Gilli, A., Grzesik, D.A., Guilderson, T.J., Muller, A.D., Bush, M.B., Correa-Metrio, Y.A., Escobar, J., Kutterolf, S., 2008. An 85-ka record of climate change in Lowland Central America. Quat. Sci. Rev. 27, 1152–1165.

Holliday, V.T. (Ed.), 1992. Soils in Archaeology: Landscape Evolution and Human Occupation. Smithsonian Institution Press, Washington, DC.

Holliday, V.T., Gartner, W.G., 2007. Soil phosphorus and archaeology: a review and comparison of methods. J. Archaeol. Sci. 34, 301–333.

Iremonger, S., Brokaw, N.V.L., 1995. Vegetation classification for Belize. Appendix to. In: Wilson, R. (Ed.), Towards a National Protected Area System for Belize. Programme for Belize, Belize City, Belize.

Jenny, H., 1994. Factors of Soil Formation: A System of Quantitative Pedology. Dover Publications, Inc., New York, NY (Reprint, with Foreword by R. Amundson, of the 1941 McGraw-Hill publication).

Kennett, D.J., Breienbach, S.F.M., Aquino, V.V., Asmerom, Y., Awe, J., Baldini, J.U.L., Bartlein, P., Culleton, B.J., Ebert, C., Jazwa, C., Macri, M.J., Marwan, N., Polyak, V., Prufer, K.M., Ridley, H.E., Sodemann, H., Winterhalder, B., Haug, G.H., 2012. Development and disintegration of Maya political systems in response to climate change. Science 338, 788–791.

King, R.B., Baillie, I.C., Abell, T.M.B., Dunsmore, J.R., Gray, D.A., Pratt, J.H., Versey, H.R., Wright, A.C.S., Zisman, S.A., 1992. Land Resource Assessment of Northern Belize. Bulletin 43. Natural Resources Institute, Kent, UK.

Lentz, D.L., Dunning, N.P., Scarborough, V., Magee, K., Thompson, K., Weaver, E., Carr, C., Terry, R., Islebe, G., Tankersley, K., Grazioso Sierra, L., Jones, J.G., Buttles, P., Valdez, F., Ramos, C., 2014. Forests, fields, and the edge of sustainability at the Late Classic Maya city of Tikal. Proc. Natl. Acad. Sci. 111, 18513–18518.

Luzzadder-Beach, S., Beach, T., 2009. Arising from the wetlands: mechanisms and chronology of landscape aggradation in the northern coastal plain of Belize. Ann. Assoc. Am. Geogr. 99 (1), 1–26.

Luzzadder-Beach, S., Beach, T., Dunning, N., 2012. Wetland fields as mirrors of drought and the Maya abandonment. Proc. Natl. Acad. Sci. 109 (10), 3646–3651.

Luzzadder-Beach, S., Beach, T., Hutson, S., Krause, S., 2016. Sky-earth, lake-sea: climate and water in Maya history and landscape. Antiquity 90, 426–442.

Luzzadder-Beach, S., Beach, T., Garrison, T., Houston, S., Doyle, J., Román, E., Bozarth, S., Terry, R., Krause, S., Flood, J., 2017. Paleoecology and geoarchaeology at El Palmar and the El Zotz Region, Guatemala. Geoarchaeology 32:90–106. http://dx.doi.org/10.1002/gea.21587.

Marshall, J.S., 2007. Geomorphology and physiographic provinces of Central America. In: Bundschuh, J., Alvarado, G.E. (Eds.), Central America, Geology: Resources and Hazards. Taylor & Francis Group, London, pp. 75–122.

Medina Elizalde, M., Burns, S.J., Polanco Martinez, J., Lases-Hernández, F., Beach, T., Shen, Chuan-Chou, Wang, Hao-Cheng, 2016. High-resolution speleothem record of precipitation from the Yucatan Peninsula spanning the Maya Preclassic Period. Glob. Planet. Chang. 138, 93–102.

Meerman, J., 2011. Belize Ecosystems (Polygon) Dataset. Belize Tropical Forest Studies. http://www.biodiversity.bz/Belize_Ecosystems_2011.zip (website last visited 12 May 2017).

Mehlich, A., 1984. Mehlich 3 soil test extractant: a modification of Mehlich 2. Commun. Soil Sci. Plant Anal. 15, 1409–1416.

Mueller, A.D., Islebe, G.A., Anselmetti, F.S., Ariztegui, D., Brenner, M., Hodell, D.A., Hajdas, I., Hamann, Y., Haug, G.H., Kennett, D.J., 2010. Recovery of the forest ecosystem in the tropical lowlands of northern Guatemala after disintegration of Classic Maya polities. Geology 38, 523–526.

Munro-Stasiuk, M., Manahan, T., Stockton, T., Ardren, T., 2014. Spatial and physical characteristics of *rejolladas* in northern Yucatán, Mexico: implications for ancient Maya agriculture and settlement patterns. Geoarchaeology 29, 156–172.

Paton, T., Humphreys, G., Mitchell, P., 1995. Soils: A New Global View. Yale University Press, New Haven, CT.

Phillips, J.D., Šamonil, P., Pawlik, L., Trochta, J., Daněk, P., 2017. Domination of hillslope denudation by tree uprooting in an old-growth forest. Geomorphology 276, 27.

Pohl, M.D., Pope, K.O., Jones, J.G., Jacob, J.S., Piperno, D.R., deFrance, S.D., Lentz, D.L., Gifford, J.A., Danforth, M.E., Josserand, J.K., 1996. Early agriculture in the Maya Lowlands. Lat. Am. Antiq. 7 (4), 355–372.

Pohl, M.E.D., Piperno, D.R., Pope, K.O., Jones, J.G., 2007. Microfossil evidence for Pre-Columbian maize dispersals in the Neotropics from San Andres, Tabasco, Mexico. Proceedings of the National Academy of Sciences. 104, pp. 6870–6875.

Schlezinger, D.R., Howes, B.L., 2000. Organic phosphorus and elemental ratios as indicators of prehistoric human occupation. J. Archaeol. Sci. 27, 479–492.

Schulze, M.D., Whitacre, D.F., 1999. A classification and ordination of the tree community of Tikal National Park, Petén, Guatemala. Bulletin of the Florida Museum of Natural History. 41, pp. 169–297.

Sheets, P., Lentz, D., Piperno, D., Jones, J., Dixon, C., Maloof, G., Hood, A., 2012. Ancient manioc agriculture south of the Cerén Village, El Salvador. Lat. Am. Antiq. 23, 259–281.

Soil Survey Staff, 2006. Keys to Soil Taxonomy. tenth ed. Natural Resources Conservation Service, United States Department of Agriculture, Washington, DC.

Sommer, M., Schlichting, E., 1997. Archetypes of catenas in respect to matter – a concept for structuring and grouping catenas. Geoderma 76, 1–33.

Stuiver, M., Reimer, P.J., Braziunas, T.F., 1998. High-precision radiocarbon age calibration for terrestrial and marine samples. Radiocarbon 40 (3), 1127–1151.

Tankersley, K.B., Dunning, N.P., Scarborough, V., Huff, W.D., Lentz, D., Carr, C., 2016. Catastrophic volcanism and its implication for agriculture in the Maya Lowlands. J. Archaeol. Sci. Rep. 5, 465–470.

Trein, Debora C., 2016. Variable Use of a Monumental Space at the Ancient Maya Site of La Milpa, Belize. Unpublished Ph.D. Dissertation. Department of Anthropology, The University of Texas at Austin, Austin, TX.

Turner II, B.L., Sabloff, J.A., 2012. Classic Period collapse of the Central Maya Lowlands: insights about human-environment relationships for sustainability. Proc. Natl. Acad. Sci. 109, 13908–13914.

Valdez Jr., F., Scarborough, V., 2014. The prehistoric Maya of Northern Belize: issues of drought and cultural transformations. In: Iannone, G. (Ed.), The Great Maya Droughts in Cultural Context: Case Studies in Resilience and Vulnerability. University of Colorado Press, Boulder, CO, pp. 255–269.

Wahl, D., Hansen, R., Byrne, R., Anderson, L., Schreiner, T., 2016. Holocene climate variability and anthropogenic impacts from Lago Paixban, a perennial wetland in Petén, Guatemala. Special issue on climate change and archaeology in Mesoamerica. Glob. Planet. Chang. 138, 70–81.

Walling, S., 2005. Archaeological investigation of Prehispanic Maya residential terraces, commoner housing and hydrology at Chawak But'o'ob, Belize. Antiquity 79, 304.

Webb, E.A., Schwarcz, H.P., Healy, P.F., 2004. Detection of ancient maize in lowland Maya soils using stable carbon isotopes: evidence from Caracol, Belize. J. Archaeol. Sci. 31, 1039–1052.

Wright, A.C.S., Romney, D.H., Arbuckle, R.H., Vial, V.E., 1959. Land in British Honduras. Colonial Research Publication No. 24. Her Majesty's Stationery Office, London, UK.